JOHANNES KEPLER
UNIVERSITY LINZ

Submitted by
Nikolas Heitzmann

Submitted at
Linz Institute for Organic Solar Cells (LIOS) / Institute of Physical Chemistry

Supervisor
o.Univ. Prof. Mag. Dr. DDr. h.c. Niyazi Serdar Sariciftci

Co-Supervisor
Dr. Dogukan Hazar Apaydin

03.2019

Electrochemical behavior of perylene derivatives and polyaniline towards CO_2 reduction

Master Thesis

to obtain the academic degree of

Diplom-Ingenieur

in the Master's Program

Technical Chemistry

JOHANNES KEPLER UNIVERSITY LINZ
Altenberger Str. 69
4040 Linz, Austria
www.jku.at
DVR 0093696

JOHANNES KEPLER
UNIVERSITY LINZ

STATUTORY DECLARATION

I hereby declare that the thesis submitted is my own unaided work, that I have not used other than the sources indicated, and that all direct and indirect sources are acknowledged as references. This printed thesis is identical with the electronic version submitted.

Place, Date Signature

Acknowledgements

First and foremost, I would like to sincerely thank o.Univ. Prof. Mag. Dr. DDr. h.c. Niyazi Serdar Sariciftci for providing me the opportunity to conduct my studies at the Linz Institute of Organic Solar Cells (LIOS) / Institute of Physical Chemistry. Throughout his inspiring lectures and fruitful words, I was able to improve my scientific abilities and sharpen my senses to look at the bigger picture of any problem.

I also want to thank my supervisor Dr. Dogukan Hazar Apaydin in this regard, who introduced me into the fascinating field of electrochemistry. His patience, knowledge, and his guidance made this thesis to what it is today. Thank you for your advices inside and outside of the laboratory that inspired me to overcome any arising challenges in my life.

Prof. Dr. Heinz Langhals helped me with the understanding and characterization of the utilized perylene derivative materials with his excellent advice and discussions. Thank you!

Special thanks also goes to my colleagues and friends Dominik Wielend MSc, Hathaichanok Seelajaroen MSc, and Wittawatt Keawsongsaeng MSc, who always supported me and had an open ear for scientific- and non-scientific discussions that made me smile and lightened up the mood in the laboratories. I was able to learn a lot about handling new analyzation methods and countless experimental approaches through you.

I want to thank every person who also helped me to facilitate this thesis: Mag. Dr. Helmut Neugebauer, Assoc. Prof. DI Dr. Markus Clark Scharber, Dr. Cigdem Yumusak, Dr. Dong Ryeol Whang, Dr. Halime Coskun Aljabour, Gabriele Hinterberger, and everyone who influenced the outcome positively in any way! Thank you all for another amazing experience and the heartwarming social environment at LIOS that I was able to be part of.

Without any doubt, I want to highlight the overwhelming support that I got from my family, like my father and mother, and their respective partner, as well as my grandparents and my relatives. Your backup and support have brought me to where I am, which is why I am deeply grateful to have you all! In addition, I want to thank each and every one of my friends and colleagues, who showed tremendous support and motivated me to become a better version of myself from day to day.

I especially want to dedicate this work to my grandfather Hermann Harrer, who passed away days before I started the practical work for this thesis. Here’s to you, a great grandfather and a man who taught me countless things but primarily to the man who knew how to keep our family together!

Abstract

The awareness of our changing environment and the potential threat of global warming has been increasing over the last decades. More and more CO_2 and other greenhouse gases are being emitted into the atmosphere by various industrial processes and moreover by the combustion of fossil fuels. Metal- and organic semiconductors have gained interest as suitable candidates for the reduction of carbon dioxide to reusable chemical fuels. Different organic materials were being investigated towards possible catalytic semiconductor behavior throughout this thesis. Carbonyl-functionalized perylene derivatives were evaporated onto glassy carbon electrode and tested for possible CO_2 capturing abilities in organic- and aqueous electrolyte solutions. Polyaniline (PANI) was electropolymerized onto glassy carbon and was subjected to a series of (photo-)electrochemical experiments in aqueous electrolyte solution, which aimed to reveal an alcohol and/or carbon monoxide product formation. A possible route of increasing the product formation was explored by the electrodeposition of copper islands (2 µm) on a PANI film, as an improved electrode. Moreover, an electro-co-polymerization of both aforementioned materials (perylenes and PANI) was attempted onto chromium-gold (Cr-Au) and glassy carbon electrodes with the intent to provide a capable electrode of capturing and/or reducing CO_2 upon demand. For the most parts, electrochemical methods like cyclic voltammetry (CV) and chronoamperometry (CA) were employed for the characterization of the materials. Furthermore, scanning electron microscopy (SEM) and infrared spectroscopy (FTIR) were utilized for a better understanding of structural changes.

Kurzfassung

Das Bewusstsein, um das sich verändernde Klima und die potentielle Gefahr der globalen Erwärmung hat sich über die letzten Jahrzehnte erhöht. Mehr denn je entweichenTreibhausgase CO_2 in die Erdatmosphäre, aufgrund der vielzähligen Industrieprozesse und vordergründig durch das Verbrennen von fossilen Treibstoffen. Metallische und organische Halbleiter gewannen an Interesse als potentielle Kandidaten, um Kohlendioxid zu widerverwertbaren chemischen Treibstoffen zu reduzieren. Verschiedene organische Materialien wurden hingehend ihres möglichen Halbleiterverhaltens in dieser Arbeit untersucht. Carbonyl-funktionalisierte Perylenderivate würde auf Glaskohlenstoffelektroden aufgedampft und in organischen und wässrigen Elektrolytlösungen hingehend ihrer Eigenschaften CO_2 aufzufangen getestet. Polyanilin (PANI) wurde auf Glaskohlenstoffelektroden elektropolymerisiert als Basis für eine Serie von (photo-)elektrochemischen Experimenten in wässriger Elektrolytlösung, die das Ziel verfolgten eine Entstehung von Alkohol- und Kohlendioxid Produktion aufzuzeigen. Dabei wurde eine mögliche Erhöhung der Produktanteile untersucht, indem Kupferinseln (2 µm) auf einem PANI-Film, als eine verbesserte Elektrode, elektrochemisch abgeschieden wurden. Darüber hinaus wurde eine elektro-co-polymerisation mit beiden Materialien (Perylene und PANI) auf einer Chromium-Gold- (Cr-Au) und Glaskohlenstoffelektrode verübt, mit der Absicht eine fähige Elektrode herzustellen, die nach Bedarf sowohl CO_2 auffangen und reduzieren kann. Hauptsächlich wurden elektrochemische Methoden wie Cyclovoltammetrie (CV) und Chronoamperometrie (CA) zur Charakterisierung der Materialien eingesetzt. Des Weiteren wurde Rasterelektronenmikroskopie (REM = SEM) und Infrarotspektroskopie (FTIR) verwendet, um ein besseres Verständnis von strukturellen Veränderungen zu erhalten.

JOHANNES KEPLER UNIVERSITY LINZ

Table of contents

1. Introduction

1.1. Background

The earth is the cradle of humanity and one of the only known planets that support life forms, to this date. Although other planets with similar estimated traits were discovered multiple lightyears away in far distant galaxies [1],[2], it is only earth that provides a viable and unique habitat for us humans. Therefore, it is in our best interest to create and maintain a sustainable environment, not only for the present but furthermore for future generations.

Constantly rising temperatures over many decades are one of the harbingers that indicate that global warming and the climate change are one of the most serious and pressing matters in today's society. The observed facts of an accelerated climate change have been identified by numerous scientific groups and are since a great motivation for a needed change towards a sustainable future [3],[4],[5]. It was found that greenhouse gases such as carbon dioxide (CO_2), methane (CH_4) and many more [6] are accountable for the enhanced rate of the climate change with their increasing emissions into the atmosphere.

One of the primary harmful greenhouse gases is CO_2, which has already reached an atmospherically concentration of ~400 ppm over a few decades [7]. It is one of the most rapidly concentrating gases in the atmosphere and is therefore an enormous concern for the environment. In addition, the life time of such greenhouse gases plays a major role, since it states the residence time that the gas will remain in the atmosphere. Hereby, CO_2 has an estimated atmospheric life time of 5-200 year. However, a specific lifetime cannot be accounted for CO_2 because of its different rates of uptake by different removal processes (ocean, forests, etc.). It is also suggested that a certain percentage of fossil carbon dioxide cannot be absorbed and will remain in the atmosphere for centuries, which makes it even a bigger concern.[8],[9],[10]

The promptly progressive industrialization and the increasingly desired wealth of the world population are predicting an increase of CO_2 emissions in the future. This can be estimated from the rapidly increasing population and the great rise on the demanded energy consumption. Until today one of the common sources of energy are fossil fuels, which are contributing via combustion of hydrocarbons (mobility, transportation, factories) to the rising CO_2 emissions.

A logical route to reduce greenhouse gas emissions and to tackle global warming is to decrease the amount of required fossil fuels and carbon-based energy resources. The goal to create a less carbon-dependent future can be achieved by providing a technological alternative that is capable of performing similar or equal to already employed standards. This problem is addressed by

advancing and enforcing the development of renewable energy technologies, such as photovoltaic, wind turbines, and water power. These carbon-free energy sources become more and more important with the rising CO_2 emissions and high energy consumption technologies, like electric cars. However, not every country has the necessary geographical requirements to produce sufficient energy from renewable sources. Therefore, the coverage of the population's energy demand cannot be fully covered yet by this approach. In theory, a massive solar plant with an area of multiple km^2 in the desert could provide enough energy to sufficiently supply Europe [11]. Nevertheless, there is still a problem between the time, the place of production, the transportation, and the utilization of this energy (Figure 1), due to ineffective technological energy storage solutions.

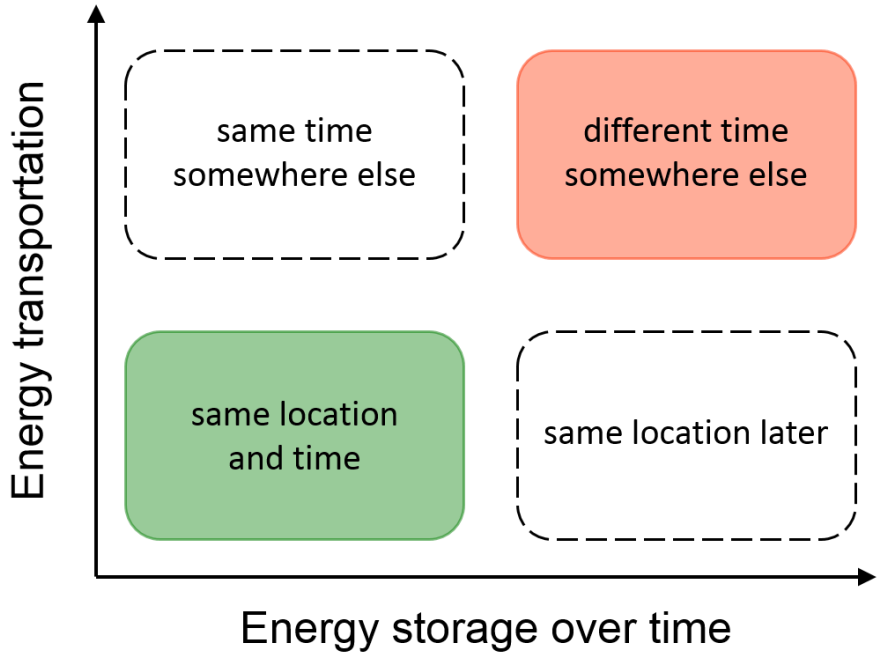

Figure 1: Schematic of the energy-transportation and -storage dilemma that arises with the production (green) and consumption (red) of energy.

It is certainly one way to tackle global warming by reducing CO_2 emissions of industrial energy generation but it will indeed take a specific amount of time until a zero-carbon emission process will be instated. We can ask ourselves, what we could do during the needed transition time from carbon-based to carbon-free energy sources and how we could use or reduce the already available amounts of CO_2 in our atmosphere and from the industry. While the efficiency of fossil fuels and the overall energy consumption is constantly refined, it is certain that we have to go further to lower global carbon emissions. There are already two prominent approaches to this problem. One describes ways to decrease the amount of CO_2 in the atmosphere by storing carbon emission gases, named carbon capture and storage (CCS). The other one called carbon capture

and utilization (CCU), deals with the conversion of carbon dioxide to more potent chemical species that can be reused.

CCS incorporates the capture of CO_2 by utilizing gas separation techniques from carbon-based electricity generation or industrial processes. The carbon dioxide is then transported by ship or through a pipeline to a location with suitable geological deposit formations. Hereby, natural hydrocarbon reservoirs, e.g. crude oil deposits, are favored because of their natural resistance for leakages. Furthermore, coal mines and saline aquifers are also mentioned as options that allow the physical storage of carbon dioxide but with very little knowledge about their reliable storing capabilities and possible leakage into the atmosphere. Nevertheless, one has to take into consideration that CCS also has its downside in terms of limited amount of natural occurring storage sites. In addition, long term studies have yet to prove that the carbon dioxide is being stored reliably and that it won't leak back into the atmosphere through natural disasters, like earth quakes and chamber eruptions. One of the biggest disadvantages is that the produced CO_2 is only stored and not utilized in any ways, which leaves it contradictory to create a long-term sustainable environment.[12]

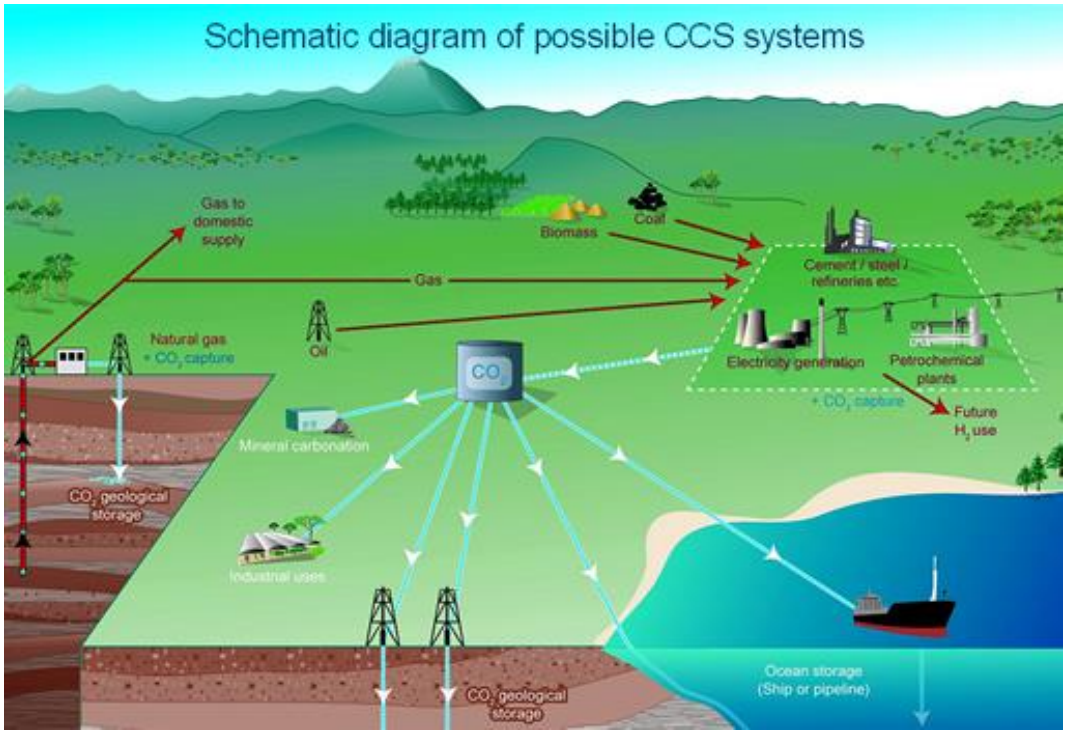

Figure 2: Schematic of possible carbon capture and storage systems. [13]

A far more refined approach is presented by CCU, where the captured carbon dioxide is regarded as a valuable carbon feedstock. The versatile C_1 carbon raw material can be utilized for the production of different chemical species, like methanol, methane, formate, and many more (Figure 3). This approach offers a better way of carbon recycling, which makes it promising for a sustainable future.[13],[14]

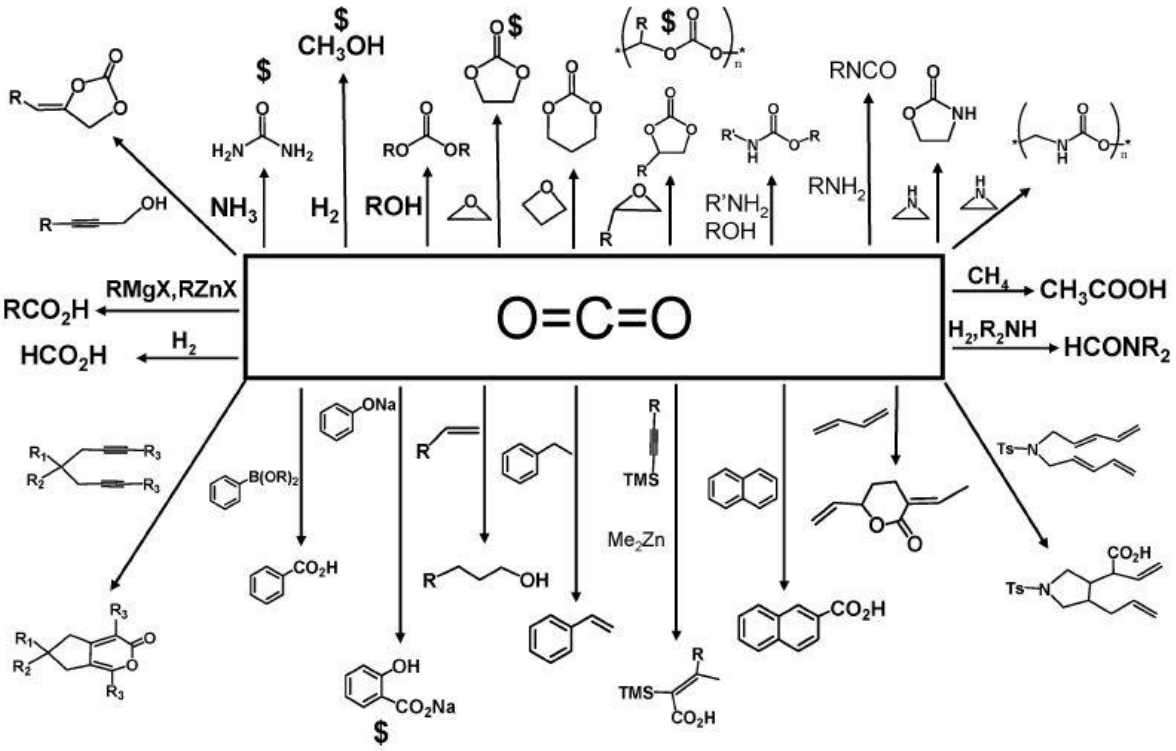

Figure 3: Scheme of all suggested reaction pathways of carbon dioxide to higher hydrocarbons.[15]

1.2. Electrochemical Carbon Dioxide Reduction Reaction

The main-idea of carbon dioxide reduction is to recycle CO_2 emissions from the combustion of fossil fuels and from the atmosphere further to chemical fuels by adding protons and electrons. The route of direct electroreduction of carbon dioxide (e.g. to hydrocarbons, CO) is attractive, since it can be combined with renewable energy resources, can be conducted at ambient pressure and temperature, and is adjustable by different electrolyte systems and by the applied voltage. Nevertheless, the field still faces multiple challenges like, the large overpotential that is required, selectivity issues for resulting products, the long-time stability of produced electrodes, high cost of noble metal catalysts, and low industrial application possibilities.[16],[17]

Carbon dioxide is a linear molecule, which is by itself an inert gas because it is thermodynamically stable. This proposes a challenge to enable an uphill reaction to other chemicals species. Overall, the kinetics and thermodynamics of the transition play a major role in the catalytic transformation. Regarding kinetics, CO_2 is converted through a one electron process to a radical carbon dioxide species. Usually this is an energetically high process, which renders it unfavorable. However, the proton-assisted electron transfer enables reactions at lower thermodynamic potentials, which can be overcome by applying an external bias. A table with possible reactions ways of carbon dioxide to various products is depicted in Table 1 with their required thermodynamic potentials.[16],[17]

$CO_2 + e^- \rightarrow \cdot CO_2^-$	$E^{0'} = -1.90$ V	(Eq.1)
$CO_2 + 2H^+ 2e^- \rightarrow CO + H_2O$	$E^{0'} = -0.53$ V	(Eq.2)
$CO_2 + 2H^+ 2e^- \rightarrow HCOOH$	$E^{0'} = -0.61$ V	(Eq.3)
$2H^+ 2e^- \rightarrow H_2$	$E^{0'} = -0.41$ V	(Eq.4)
$CO_2 + 4H^+ 4e^- \rightarrow HCHO + H_2O$	$E^{0'} = -0.48$ V	(Eq.5)
$CO_2 + 6H^+ 6e^- \rightarrow CH_3OH + H_2O$	$E^{0'} = -0.38$ V	(Eq.6)
$CO_2 + 8H^+ 8e^- \rightarrow CH_4 + H_2O$	$E^{0'} = -0.24$ V	(Eq.7)

Table 1: Known conversion routes of carbon dioxide with the required thermodynamic potentials vs. NHE at pH 7.

The shown potentials in Table 1 are given for a normal hydrogen electrode (NHE), which is per definition the standard reference point for standard electrochemical reduction potentials, with an assigned potential E^0 as 0 V. Moreover, the reference electrode must have 1 atm of hydrogen and a hydronium ion activity of 1. However, these parameters may vary for each experimental setup, which is why they have to be adjusted according to the Nernst equation. It is common to state the potential vs. a reversable hydrogen electrode (RHE), which takes in addition to the NHE the pH of the solution into account.[18] The electrochemical reduction process is especially sensitive in aqueous electrolyte solution due to the side reaction of hydrogen evolution, which is competing with the CO_2 reduction on the same cathode. Furthermore, the similar redox potentials for the multiple reduction pathways in Table 1 lead to the formation of multiple products, which is why a suitable carbon dioxide reduction electrocatalyst has to be instated to achieve a high selectivity and therefore a high effective electrochemical system.[16],[17]

Catalysis is a wide-ranging scientific field that has been studied and researched for many decades by numerous famous scientists. It can be divided into two categories named homogeneous and heterogeneous catalysis. Homogeneous catalysis describes the reaction of a catalyst with educts in the same physical phase, which is mostly in the liquid-liquid phase for CO_2 reduction catalysts. A famous example for a same-phase catalyst is the Lehn catalyst, which is a metal bipyridine complex. Lehn and Ziessel [19] initially worked on the development of one of the first photochemical active CO_2 reducing metal catalyst. Later on, Hawecker, Lehn, and Ziessel presented the advanced reactivity of Ru- and Re-complexes [20],[21], whereas the metal complex know as Lehn catalyst, which has a bipyridine- and a chloide-ligand is discussed in their paper in 1984 [21]. Sullivan *et al.* suggested a reaction mechanism for the activation of the catalyst and the conversion from CO_2 to CO [22]. Although homogeneous catalysts can provide a high selectivity and an adequate way of fine-tuning the catalysts properties, it is not predominantly used in industrial processes because of high catalyst recycling costs and the narrow condition window that it can be utilized in [23].

Besides some disadvantages that have to be faced with the utilization of heterogeneous catalysts, they are outperforming homogeneous catalysts in a wide variety of industrial applications. Many industrial processes today rely on heterogeneous catalysis applications that enables them at first hand and makes them profitable at second hand. There are numerous inorganic and organic catalyst systems known in this scientific field, which are potent enough to reduce carbon dioxide into various chemical fuels.

Polyaniline (PANI) is an exceptional material that has been investigated towards electrochemical carbon dioxide reduction over the last decades. The utilization of bare polymer electrodes without any supporting metal catalyst are favored because of their low production costs. One of the first polyaniline-only electrodes were tested by Aydin *et al.*[24] under ambient and high pressure conditions in an methanol electrolyte. A maximal potential of - 0.4 V (vs. SCE) was utilized, which yielded formaldehyde, formic acid and acetic acid as products. Later on, Köleli *et al.*[25] worked with a bulk PANI-electrode and a membrane cell in a methanol electrolyte at ambient conditions, which produced formic acid and acetic acid at an electrolysis potential of - 0.4 V vs. SCE.[26]
The publication of a recent paper from Hursán *et al.*[27] reports a successful photoelectrolysis of an polyaniline/glassy carbon electrode in a 0.1 M sodium sulfate aqueous electrolyte solution. The publication reveals a total product formation of 20 % faradaic efficiency (FE) for hydrogen, 43 % FE for methanol and 20 % FE for ethanol production at an electrolysis potential of - 0.4 V vs. Ag/AgCl/3M NaCl. These results promise a new approach to the electrochemical reduction capabilities of polyaniline, since most literature that is found deals with carbon dioxide reduction in organic solvents (e.g. methanol), rather than aqueous electrolyte solutions [26],[28]. Therefore, an increased focus is set on the photoelectrochemical reduction of carbon dioxide with bulk-conductive polymer electrodes in aqueous electrolyte solution.

A major drawback of bulk polymer electrodes is the low efficiency, besides the poor selectivity and catalytic properties. Therefore, modern electrochemical systems with a supporting metal catalyst (e.g. copper) were already subject of investigation mostly for C_1, C_2, and alcohol product formation. An early publication was made by Ogura *et al*.[29] who electrochemically investigated a Prussian blue and PANI laminated Pt electrode. Found products included lactic acid, formic acid, acetic acid, as well as methanol and ethanol. Grace *et al.*[30] studied the behavior of an PANI electrode with electrodeposited Cu_2O nanoparticles incorporated in an 0.1 M tetrabutylammonium perchlorate (TBAP) and methanol electrolyte solution. An electrolysis at - 0.3 V vs. SCE revealed a 30.4 % FE for formic acid and 63.0 % FE for acetic acid.[26]

A special focus in this work is directed towards heterogeneous catalysis with organic pigments and polymers in aqueous electrolyte solution. Polyaniline electrodes are employed as conductive

polymers, whereas different carbonyl-functionalized perylene derivatives are utilized to attempt an improvement of the interaction of the catalyst with the carbon dioxide. Different applications for perylene derivatives are known to be field effect transistors [31],[32], solar cells [33],[34], and photoanodes for oxygen evolution [35]. The interesting story about these pigments is the capability of electrochemically capturing and releasing CO_2. Apaydin *et al.* utilized an immobilized naphthalene bisimide pigment to electrochemically capture and release carbon dioxide, over its reduced carbonyl groups of the material.[36] Liao *et al.* presented that synthesized polyimide networks can be made from melamine and perylene-3,4,9,10-tetracarboxylic dianhydride (PTCDA), which showed an CO_2 uptake of up to 15 wt %.[37] Improved version of such porous polyimide networks was done by Rao *et al*., which achieved a total uptake of 43 wt %.[38] Burian *et al.* proved that carbon dioxide capture was also achievable by processing perylene bisimide hydrogels. The literature on the electrochemical properties of perylenes [39],[40] makes it an interesting topic for further investigation, especially in the reductive potential regime. However, a way of interlinking the polyaniline-chains and perylene derivatives (e.g. PTCDA) in an attempted electro-co-polymerization is conducted in this thesis to observe possible CO_2 capture and/or reduction properties.

1.3. A glimpse into the past and present of polyaniline

Polyaniline is a conductive and nitrogen rich polymer that is made through the oxidative polymerization of multiple aniline monomers. The properties of this material (e.g. conductivity) can be diverse depending on the oxidation state of the polymer and the degree of doping. PANI is regarded as one of the oldest known polymers among the common conjugated organic polymers like polyacetylene, polythiophene, polyphenylene, polypyrrole, and polyphenylenevinylene.[41] However, the conductive nature of PANI was not revealed until the work of Don Weiss in 1963 [42],[43],[44], who continued the research of great pioneers that worked before on the fundamentals of this polymer material.

The study of the monomer aniline started a long time ago in 1826 [45] where Otto Unverdorben conducted a dry distillation of indigo and isolated aniline. He obtained an oil, which he called *crystallin*. Friedlieb Ferdinand Runge isolated aniline out of coal tar as a peculiar substance in 1834 [46], which turned aquamarine upon treatment with chlorine of lime. Due to this color response he named it *kyanol*, which is a combination of the Greek word *kuanós* (blue) and Latin *oleum* (oil). In 1840 [47], Carl Julius Fritzsche treated indigo with a highly concentrated solution of base, which yielded after some further purification a colorless oil that he called *anilin*. The first connection between the discovered substances *crystallin* from Otto Unverdorben and *kyanol* from Friedlieb Ferdinand Runge was drawn by an editor of the *Journal für praktische Chemie* named Otto

Erdmann in 1840, who became aware of the similarities by reading the publication of Carl Julius Fritzsche and noting them.[47] Nikolay Zinin described two years later in 1842 [48] the reduction of nitrobenzene to a chemical species that he called *benzidam*, which was identified shortly later as *anilin* by Carl Julius Fritzsche, which he stated in a note under Zinin's publication. It was a year later in 1843 [49] when August Wilhelm Hofmann proved once and for all that the previous discovered substances *crystallin*, *kyanol*, *anilin*, and *benzidam* were in fact one and the same chemical, which was then referred to as *phenylamine* or *aniline* ever since.[41]

In 1871 [50], the word *aniline black* was mentioned the first time, which was the first general name for polyaniline and referred to the multiple black dyes that were made out of aniline. The pioneers in the field of polyaniline colors were F. F. Runge [51] (1834) and C. J. Fritzsche [47] (1840), who actively experimented with the oxidation of aniline with various chemicals to obtain dark-blue and dark-green colors. The idea of the utilization of polyaniline as a dye in industrial applications was further carried on by Crace Calvert, Samuel Clift, and Charles Lowe. They explored the vibrant green and blue color of polyaniline throughout the oxidation of aniline to find a suitable colorant for cotton and filed a patent in 1860 [52]. This green color was given the name *emeraldine*, while the blue color was named *azurine*.[41] Later on they hired the printer Wood and Wright for the production of their green and blue colors. After a few improvements they commercialized a dark shade color, which can be resembled to black.[53],[54] Nearly at the same time John Lightfoot was experimenting with a profitable roll application of the green and black aniline dyes, whereas he used besides known oxidants an additional copper salt in his final formulation, which achieved a very dark blue or green dye similar to the previously reported color of F.F. Runge. However, his dye was seen superior [53] to that of Wood and Wright, which is while he filed a patent in 1863. The recipe was improved in 1864 by Charles Lauth, who used the insoluble copper sulfate because of previously experienced roller corrosion in the fabrication.[52],[55]
Heinrich Caro worked in 1860 for Roberts, Dale & Co., where he found a black residue after the oxidation of aniline with copper salts and the extraction with alcohol of a desired purple color. The black dye was commercialized for purchase to printers and applicable with wooden hand blocks onto cotton, around at the same time as J. Lightfoot worked on his aniline black recipe.[52],[55],[56]
The first known electrolysis procedure of aniline sulfate was conducted by Henry Letheby in 1862 [57], who used a sulfuric acid solution with aniline and a Pt electrode to create a blue-greenish film.

The various chemical structures and oxidation states of polyaniline were not fully explored until the propose by Arthur Georg Green and Arthur Edmund Woodhead in 1910 [58],[59],[60] with their characteristic names. Although C. J. Fritzsche discovered already the empirical formula of the emeraldine salt (Figure 5) in 1843, it was G. G. Green and A. E. Woodhead who fully described all oxidation states of the polymer.[61] The three primary forms are the fully reduced and colorless

leucoemeraldine, the half-reduced *emeraldine* that has a violet-blue color, and the fully oxidized and purple *pernigraniline*. All described oxidation states of polyaniline can be seen in Figure 4 bellow.

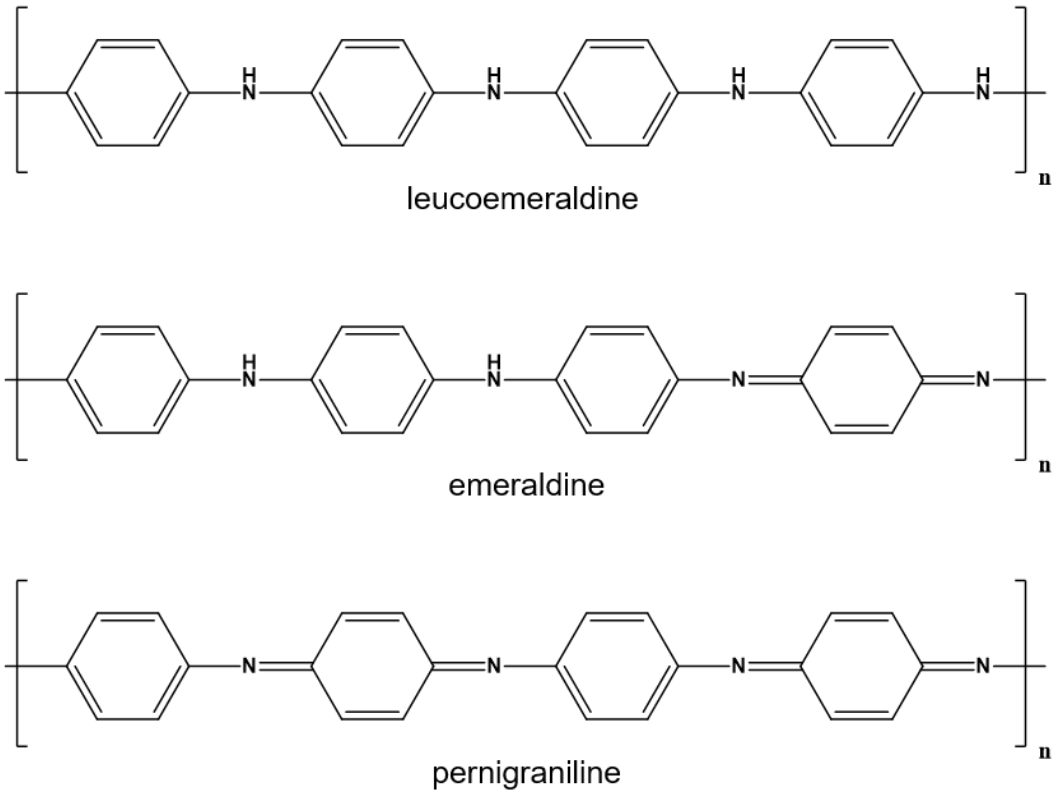

Figure 4: Three primary oxidation states of polyaniline.

Polyaniline is a special conjugated polymer because of its unique behavior in terms of conductivity, which can be adjusted via oxidative doping as well as protonation. The latter doping effect is controlled with the pH of the acid solution, which is why it is referred to as protonic acid doping. [62],[63],[64] A prime example for this doping effect is displayed in Figure 5 for the commonly known green emeraldine salt of polyaniline.

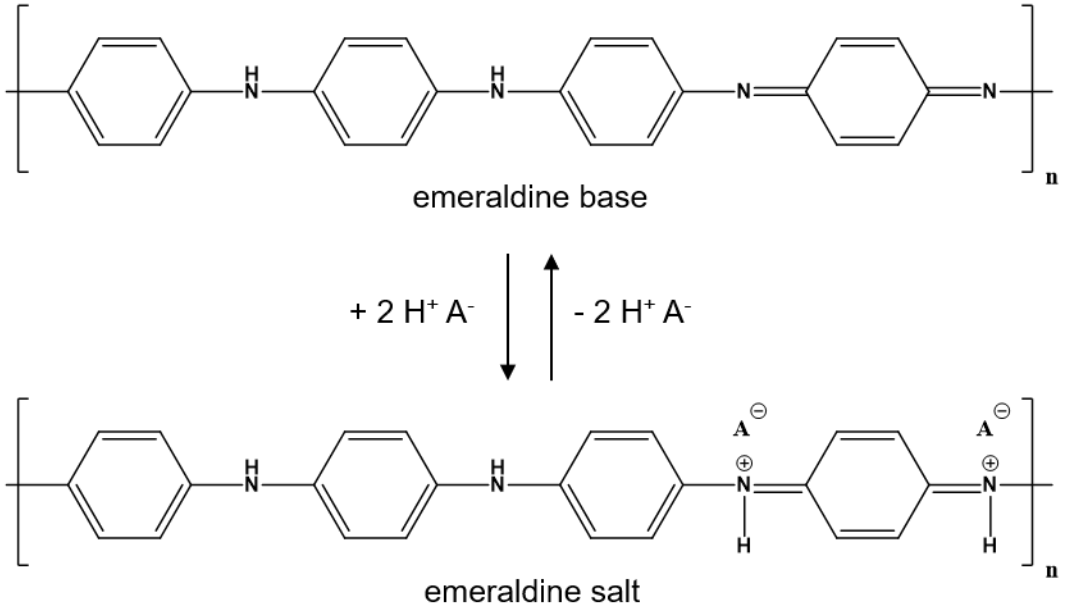

Figure 5: Protonic equilibrium of the emeraldine base (blue-violet) and emeraldine salt (green).

The shown emeraldine salt (Figure 5) is the most conductive oxidative state of polyaniline that can be achieved. PANI is generally synthesized via an oxidative polymerization in very acid aqueous media, whereas an electrochemical- and chemical polymerization can be utilized.[65],[66]

In case of the electrochemical synthesis of polyaniline, a potentiostatic, potentiodynamic, or galvanostatic method is employed for the deposition of the material.[66],[67] Parameters like pH of the electrolyte, electrode material, dopant anions = electrolyte composition, and applied potential have an enormous influence on the polymerization process and therefore on the quality of the produced polymer.[68] Start of the polymerization is induced by the formation of an anilinium radical cation via the oxidation of monomers on the electrode.[68],[69],[70] Control of the applied potential is crucial in order to receive the desired oxidation state of the polymer and to avoid an overoxidation of the material, which leads to defects such as crosslinking or formation of paraquinones.[66],[71]

Chemical polymerization of PANI is a major technique for commercial produced bulk powders, coated products and dispersions. An additional chemical oxidant like aqueous ammonium persulfate has to be employed that provides enough oxidizing force. Important process parameter are the type/concentration of oxidizing agents, utilized protonic acids, pH of the solution, aniline/oxidant ratios, and the temperature during the polymerization.[66],[71] Besides ammonium persulfate, other oxidizing agents like $FeCl_3$ (mainly for organic solvents) can be used. Different aqueous solutions of sulfuric acid or hydrochloric acid are employed to provide their respective anions and to keep the pH < 3 in order to dissolve the monomers and to avoid side reactions.[63],[66],[67],[71]

Due to the unique properties and the time that polyaniline remained in the focus for fruitful scientific investigations, various applications have been explored for this material. The diversity of

applications ranges from solar cells to electrode for batteries but also to conductive inks, paints, and colors for textiles. However, gas-/bio-sensors, membranes for gas separation and diodes with incorporated polyaniline were reported as well.[67],[70]

1.4. Aim of this thesis

This study aims to combine the properties of PANI as a photoelectrocatalyst for CO_2 reduction and the perylene derivatives as enhancer for CO_2 capture. Many materials with carbonyl-groups have been positively tested towards carbon dioxide capture, which is why tetracarbonyl-functionalized perylene derivatives were chosen. The publication of Hursán *et al*.[27] shows an interesting photocatalytic behavior of polyaniline in aqueous electrolyte solution at low reductive potentials. An effort was made to optimize and improve the experimental conditions to enhance the product formation at higher potentials.

2. Experimental

2.1. Materials

As mentioned in the introduction part, various tetracarbonyl perylene derivatives were subject of investigation in this thesis. The chemical structure of all 3 materials is depicted in Figure 6.

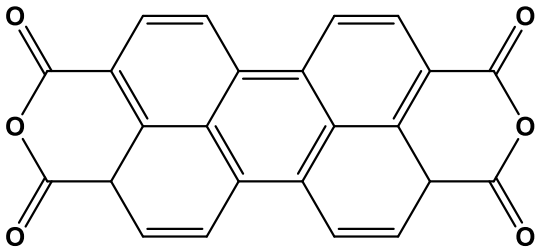

Perylene-3,4,9,10-tetracarboxylic dianhydride (PTCDA)

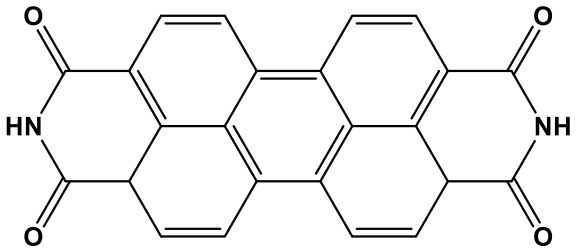

3,4,9,10-Perylene-tetracarboxylic diimide (H_2PTCDI)

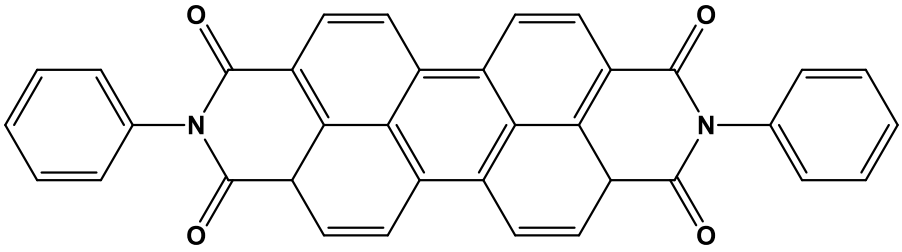

N, N'-Diphenyl-3,4,9,10-perylenedicarboximide (Diphy-PTCDI)

Figure 6: Chemical structure of all utilized perylene derivatives.

The chemical utilities such as gases, solvents, and in-/organic materials, which were used throughout this thesis are summarized in the following Table 2.

Material	Supplier	Purity	Abbreviation
3,4,9,10-Perylene-tetracarboxylic diimide	TCI	> 95.0 %	H_2PTCDI
Acetone	VWR Chemicals	technical	-
Acetonitrile	Roth	> 99.9 %	MeCN
Aniline	Sigma Aldrich	> 99.5 %	-
Carbon dioxide	Linde	99.995 %	CO_2
Chromium on tungsten rod	Kurt J. Lesker	99.9 %	-
Copper sulphate pentahydrate	Sigma Aldrich	> 99.0 %	-
Dibasic potassium phosphate	Sigma Aldrich	≥ 98.0 %	-
Glass	Thermo Scientific	Pre-cleaned	-
Glassy Carbon electrode, 2 mm	Alfa Aesar	type 1	GCE
Gold	Ögussa	99.99 %	-
Hellmanex solution	Hellma-Analytics		-
Isopropanol	VWR Chemicals	AnalaR Normapur	IPA
Mono potassium phosphate	Sigma Aldrich	> 99.7 %	-
N, N'-Diphenyl-3,4,9,10-perylenedicarboximide	Sigma Aldrich	98.0 %	Diphy-PTCDI
Nitrogen	JKU	-	N_2
Perylene-3,4,9,10-tetracarboxylic dianhydride	Fluka	purum	PTCDA
Potassium bicarbonate	Sigma Aldrich	≥ 99.5 %	-
Potassium hydroxide	Alfa Aesar	85 %	-
Silver wire, 0.5 mm diameter	Roth	99.9 %	-
Sodium sulphate anhydrous	Sigma Aldrich	> 99.0 %	-
Sulfuric acid	J. T Baker	95 – 97 %	-
Tetrabutylammonium hexafluorophosphate	Sigma Aldrich	> 99.0 %	$TBAPF_6$

Table 2: Chemicals used for conducted experiments.

2.2. Material preparation

2.2.1. Purification of crude materials

The commercially purchased materials PTCDA and H_2PTCDI were purified via sublimation in a tube furnace. Therefore, 0.5 g of crude material was transferred into a test tube, which was positioned inside of a quartz tube. The tube was sealed and preheated to 150 °C for 25 minutes before a vacuum of 10^{-2} mbar was applied for 30 minutes by an *Edwards RV12* roughing pump. Afterwards, the temperature was increased to 330 °C and the *Pfeifer Vacuum* turbo pump was switched on, which allowed to reach a stable pressure of 10^{-4} mbar after one hour. The crude material was then sublimed at a constant temperature of 350 °C for PTCDA, and 380 °C for H_2PTCDI, for four hours respectively. The purified material was then obtained by collecting the powder on the inside of the test tube. This process was repeated multiple times to yield 0.5 g of purified material, which was then sublimed a second time.

2.2.2. Cleaning of FTO and glass substrates

The cleaning of all utilized glass and FTO substrates was carried out by the following standard procedure. Unprocessed substrates were cleaned by sonication in acetone, 2% Hellmanex solution, deionized water, and isopropanol, for 15 minutes each. Afterwards, the substrates were blow dried with nitrogen gas and stored in a dust free environment.

2.3. Electrode preparation

2.3.1. Chromium-Gold- and glassy carbon electrode preparation

Chromium-Gold (Cr-Au) electrodes were produced by cutting 0.6 x 10.0 cm substrates from optical carrier glass, which were then cleaned according to the standard procedure described previously. The cleaned glass substrates were then plasma treated with a *Plasma ETCH P25* plasma oven under O_2 atmosphere with 50 W for 5 minutes. The treated substrates were then brought into a thermal evaporator, in which 5 nm of chromium and 80 nm of gold were thermally evaporated onto the substrates under high vacuum.

Glassy carbon electrodes were prepared by rinsing with MQ water and acetone before being polished with *Buehler* Al_2O_3 polishing paste for 60 seconds on each side with particle sizes ranging from 1 µm to 0.3 µm to 0.05 µm. The electrodes were sonicated for 15 minutes in MQ water and isopropanol between each different particle size. Afterwards, an additional polishing step with toothpaste was conducted to remove all remaining metal oxide particles, followed by sonication.

The activation of the glassy carbon was done electrochemically in 0.5 M H_2SO_4 with a platinum (Pt) wire as counter electrode (CE) and an Ag/AgCl/3M KCl reference electrode (RE). A potential sweep from +1500 mV to -1000 mV was applied with a scan rate of 50 mV s^{-1} for 30 cycles.

2.3.2. Organic thin film deposition

Thin films of PTCDA, H_2PTCDI, and Diphy-PTCDI were deposited onto Cr-Au and glassy carbon electrodes via thermal evaporation in a *Vaksis Organic Material Evaporator* system. PTCDA and H_2PTCDI were purified via two times sublimation beforehand and the commercial Diphy-PTCDI was directly used as source material. Hereby, 100 nm of an organic film were deposited with an evaporation rate of 0.1 nm s^{-1} and a pressure of $6 \cdot 10^{-6}$ mbar, whereas a maximum evaporation temperature of 340° C for PTCDA and Diphy-PTCDI, and 384° C for H_2PTCDI was necessary.

2.3.3. Electropolymerization of Aniline

The electropolymerization of aniline was conducted in an aqueous acidic electrolyte solution such as H_2SO_4 with concentrations ranging from 0.5 M to 1 M and aniline concentrations ranging from 25 mM to 0.1 M. The setup consisted of a Cr-Au or glassy carbon electrode as working electrode (WE), a platinum wire as counter electrode, and a quasi Ag/AgCl or saturated calomel electrode (SCE) as reference.

The later developed standard procedure included dissolving freshly distilled aniline (0.1 M, 137 µL) in 15 mL of 0.5 M H_2SO_4 while stirring. The solution was purged for 1 h with nitrogen and then a polyaniline (PANI) film was potentiodynamically electropolymerized onto glassy carbon as a working electrode, Pt foil as counter electrode and SCE as reference electrode. During the polymerization a potential from 800 mV to -200 mV with a starting potential of 350 mV and a scan rate of 25 mV s^{-1} was applied for 25 cycles. Afterwards, the electrode with the PANI film was washed by dipping it multiple times in MQ water, followed by blow drying the polymer film with compressed nitrogen.

2.3.4. Copper island deposition

Potentiostatic deposition of copper islands was conducted onto electrodes according to Luo *et al.*[72]. Hereby, a 10 mM $CuSO_4$ in 0.1 M Na_2SO_4 electrolyte was purged for 1 h with nitrogen before applying -361 mV vs. a Ag/AgCl/3M KCl reference electrode with Pt foil as counter electrode for 480 s.

2.3.5. Preparation of quasi Ag/AgCl reference electrodes

Ag/AgCl reference electrodes were prepared by grinding silver wires with 240 grid SiC sandpaper and rinsing them with MQ water. The silver wires were dipped into a beaker with 1 M HCl with an Ag/AgCl/3M KCl reference electrode and Pt foil as counter electrode. AgCl was electrochemically deposited by applying a potential sweep from 700 mV to -200 mV with a scan rate of 10 mV s^{-1} for 10 cycles. Afterwards, a potential of 300 mV is applied for 2 minutes, followed by 700 mV for 15 minutes. The finished electrodes were washed with MQ water and dried.

2.4. Electrode characterization

2.4.1. Scanning Electron Microscopy (SEM)

A *JEOL JSM-6360 LV* scanning electron microscope was used to conduct all the SEM measurements. The machine was operated at 7 kV to measure the surface structure of prepared Cr-Au and glassy carbon electrode films.

2.4.2. Attenuated total reflection infrared spectroscopy (ATR-FTIR)

The *Bruker Vertex 80* FTIR spectrophotometer equipped with a platinum ATR module was used for standard attenuated total reflection (ATR-FTIR) measurements. Measurements were usually performed with 32 averaging scans and from 5000 cm^{-1} to 500 cm^{-1}.

2.4.3. UV-Vis spectroscopy

The UV-Vis measurements were carried out with a *Perkin Elmer Lambda 1050* machine. Hereby, the adsorption of solutions in quartz cuvettes and thin films on transparent substrates (FTO) were measured from 250-800 nm.

2.4.4. Photoluminescence

Photoluminescence (PL) spectra were recorded on a *Photon Technology International* machine, equipped with double grating input and output fluorometer. A xenon short arc lamp (UXL-75XE, Ushio) was utilized for excitation and a photon multiplier tube (PMT) as detector.

2.4.5. Electrochemical characterization

All electrochemical measurements were conducted with a *Jaissle Potentiostat-Galvanostat IMP 88 PC-10*. Hereby, cyclic voltammetry (CV) was used for the characterization of organic films, on different substrates, and in different electrolytes solutions.

Electrocatalytic investigations were done in a two-compartment cell with a total volume of 52.2 mL, which was filled with 20 mL of electrolyte solution. As depicted in Figure 7, a Pt foil was used as counter electrode and an Ag/AgCl/3M KCl reference electrode, whereas Cr-Au or glassy carbon was used as working electrode. Electrolyte solutions such as 0.1 M Na_2SO_4, 0.1 M phosphate buffer pH 7 and 0.5 M potassium bicarbonate were used with this setup.

Figure 7: Utilized electrochemical cell for CV measurements in aqueous electrolyte with a Ag/AgCl/3M KCl reference electrode (RE) (left), Pt-foil as counter electrode (CE) (right), and a PTCDA/Cr-Au working electrode (WE) (middle).

Photoelectrocatalytic measurements were also conducted in a two-compartment cell with a total volume of 260 mL of which 125 mL were filled with electrolyte solution. The standard electrode arrangement included a glassy carbon electrode with a polymer film as working electrode, Pt foil as counter electrode, and an Ag/AgCl/3M KCl reference electrode. Figure 8 shows the utilized cell with an additional circular window opening for an installed quartz glass, which was needed to illuminate the active material with UV-light.

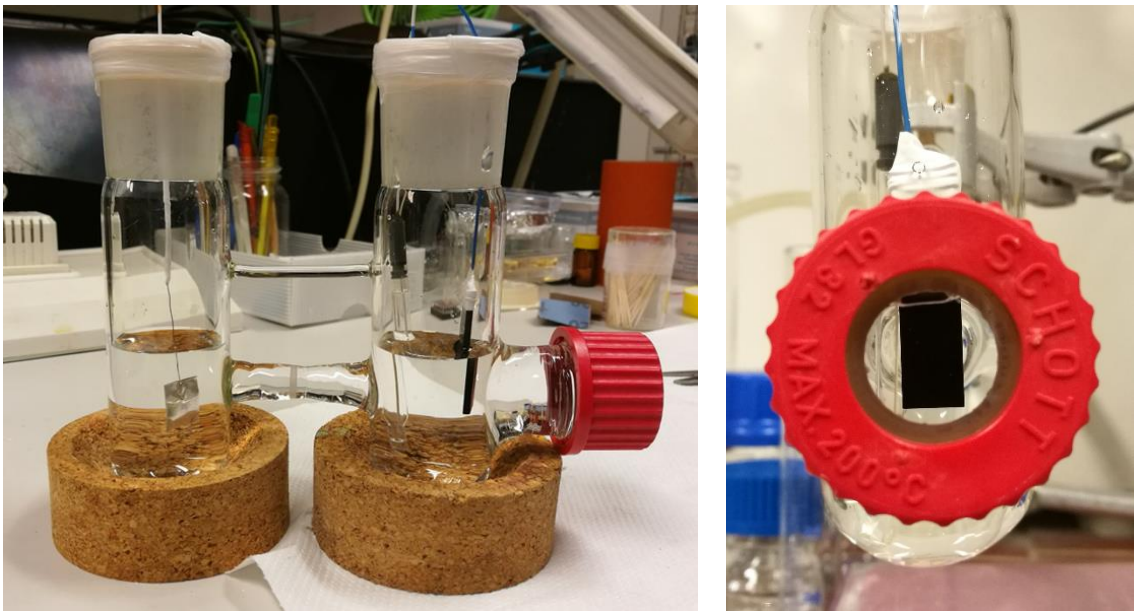

Figure 8: Utilized photoelectrochemical cell for CV measurements in aqueous electrolyte with a Ag/AgCl/3M KCl electrode (RE), Pt-foil (CE), and glassy carbon electrode (WE) (left). Opening of the quartz glass window for sample illumination (right).

The photo-assisted catalytic behavior was investigated with two different lamp setups, which were both equipped with a water filter to eliminate any heating effects. The first setup utilized a Xenon lamp with an output of 80 mW cm^{-2} while the second setup had an Hg arc lamp with the output of approximately 460 mW cm^{-2}, while applying 20 amperes. Both setups are depicted in Figure 9.

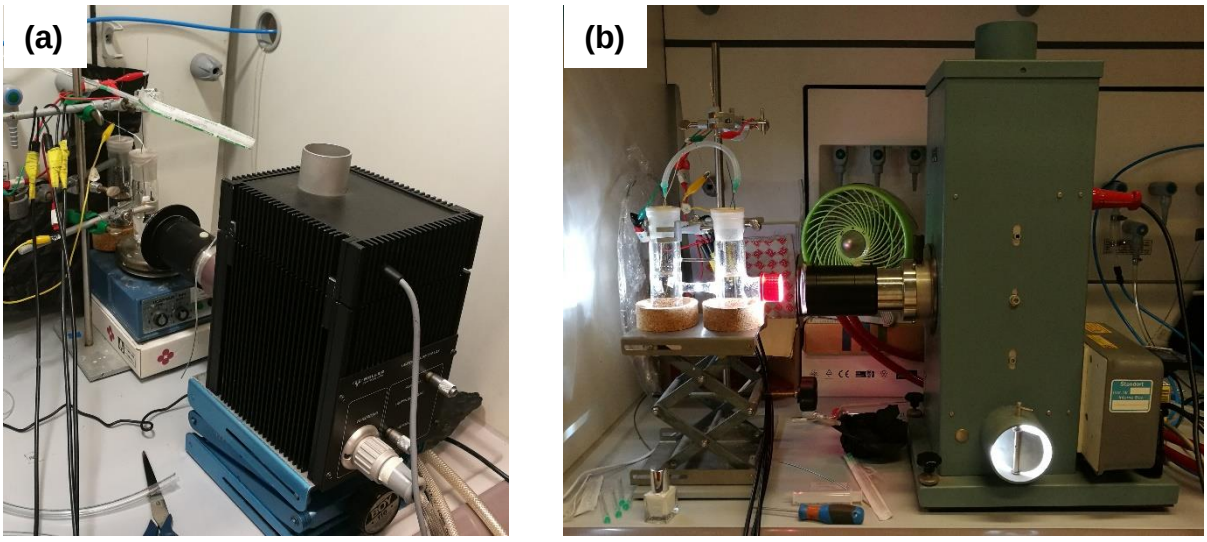

Figure 9: (a) Utilized photoelectrochemical setups with a total power output of 80 mW cm^{-2} and (b) 460 mW cm^{-2}.

2.5. Product quantification

2.5.1. Gas injection gas chromatography

The identification and quantification of gaseous samples were done with a *Thermo Scientific Trace GC Ultra* gas chromatograph by injecting 2 mL of gas sample with a gas-tight syringe into the machine, which had two distinctive channels. The left channel, which operated with nitrogen as carrier gas, was used to analyze carbon monoxide (CO), as well as methane (CH_4). The right channel was operated with helium and was primarily used for the analysis of hydrogen (H_2) gas. Both channels were operated with the same temperature program, which is shown in Table 3, whereas the detection of all analytes was done with a thermal conductivity detector (TCD).

Thermo Scientific Trace GC Ultra	
32 °C	hold for 2 min
32 - 130 °C	10 °C/min
130 °C	hold for 10 min

Table 3: Temperature program for the conducted GC measurements.

2.5.2. Ion chromatography

Liquid analytes, such as formate, were analyzed with an *ICS-5000 Dionex* ion chromatograph, which was equipped with a *Dionex Ion Pac AS19* column. The column was operated at a constant temperature of 30 °C with a flow rate of 0.25 mL min^{-1}. A conductivity detector (CD) was utilized for analyte detection. The concentration of the KOH eluent is given in Table 4.

ICS-5000 Dionex	
0 – 7 min	10 mM KOH
7 – 14 min	100 mM KOH
14 – 27 min	10 mM KOH

Table 4: KOH eluent-concentration in the IC over time.

2.5.3. Liquid injection gas chromatography

Analytes in the electrolyte solution were analyzed with a *Thermo Fischer Tracer 1310* gas chromatograph. Therefore, a TR-V1 (30 m x 0.25 mm ID x 1.4 µm film) column was loaded with 1 µL of a prepared electrolyte sample with a dilution ranging from 1:20 to 1:50 in a splitless mode.

A flame ionization detector (FID) was employed to detect gaseous analytes with the following temperature program (Table 5).

Thermo Fischer Trace 1310	
40 °C	hold for 2 min
40 – 80 °C	5 °C/min
80 – 250 °C	15 °C/min

Table 5: Temperature program for the conducted liquid injection GC measurements.

3. Results and discussion

3.1. Carbon capture properties

This chapter discusses the CO_2 capture abilities of PTCDA, H_2PTCDI, and Diphy-PTCDI films on Cr-Au and glassy carbon electrode in various electrolyte solutions. Furthermore, the effects of additional polyaniline to each material as a mediator polymer is shown.

3.1.1. PTCDA

PTCDA is a perylene derivative with two dicarboxylic-dianhydride groups attached to the perylene backbone, which can be seen in Figure 10. The color of this commercially available material is red-orange color, which can be referred to a rust tone. Compared to the other utilized derivatives, PTCDA represents the basic material from which the others can be synthesized.[73],[74] Therefore, it is investigated towards CO_2 capture because of its high abundancy and low-cost synthesis procedure.

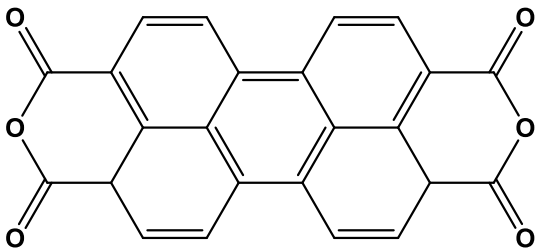

Figure 10: Chemical structure of PTCDA.

A PTCDA/Cr-Au electrode with 100 nm active film thickness was first investigated in an organic electrolyte solvent, such as 0.1 M tetrabutylammonium hexafluorophosphate ($TBAPF_6$) salt in acetonitrile. Hereby, the PTCDA/Cr-Au electrode was the working electrode, a Pt wire was the counter electrode, and a quasi Ag/AgCl was used as a reference electrode. The corresponding CV can be seen in Figure 11.

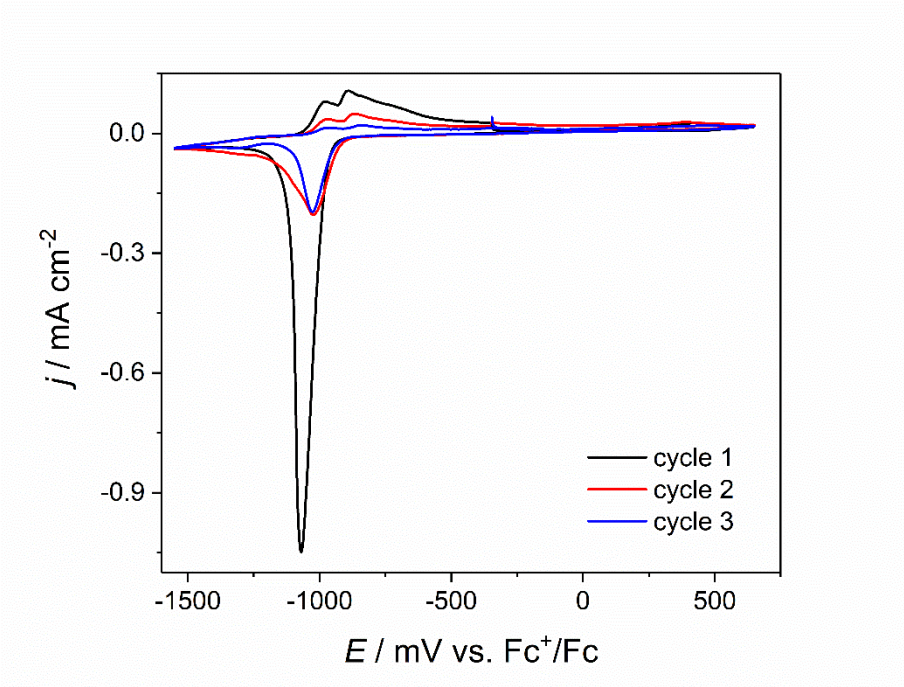

Figure 11: PTCDA on Cr-Au in 0.1 M $TBAPF_6$ / MeCN under N_2.

The same oxidative and reductive peaks were observed upon comparison of the individual cycles in Figure 11. However, it was noticed that the pink material was partially dissolved during the experiment at the first reduction peak, which changed the color of the electrode to yellow and was restored to some extent to pink after reoxidation. The decreasing current density was hereby a result of the progressive dissolution of PTCDA into the electrolyte with increasing number of cycles, which was the reason why no further investigations under CO_2 were conducted.

Further experiments in aqueous electrolytes were carried out with a focus to ensure the stability of the material during measurements. A 0.1 M Na_2SO_4 electrolyte solution was therefore used to measure the electrochemical behavior of a PTCDA/Cr-Au electrode. Nevertheless, the material was dissolved as well after the first reduction peak into the electrolyte. Moreover, a 0.1 M phosphate buffer (pH 7) was chosen for further electrochemical experiments to eliminate the dissolution of the pigment which might arise from a pH change as a result of CO_2 purging. The resulting CV of a fast screening experiment with a PTCDA/Cr-Au electrode can be seen in Figure 12.

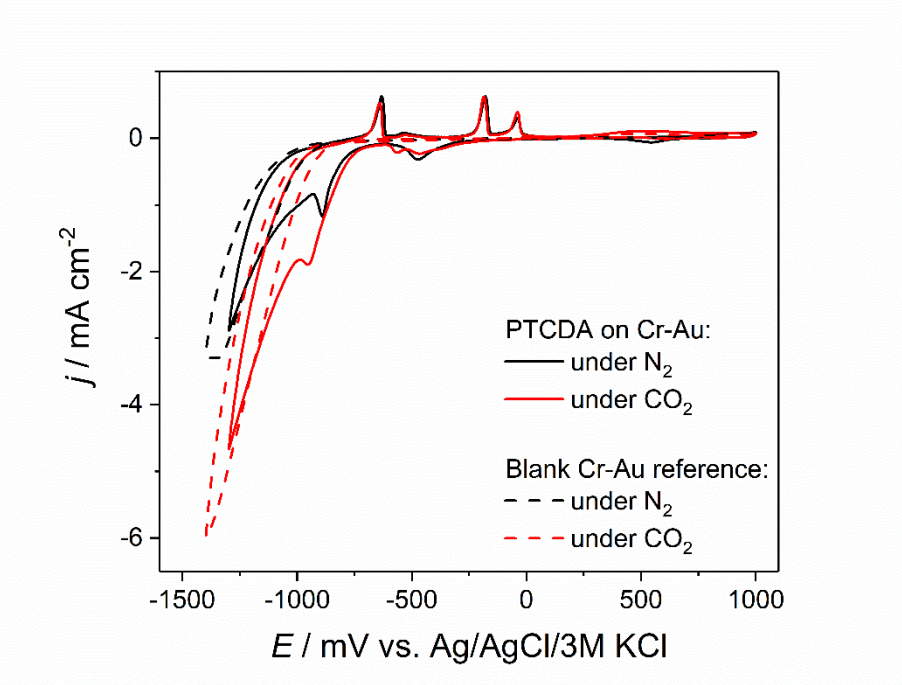

Figure 12: PTCDA on Cr-Au in 0.1 M phosphate buffer (pH 7) under N_2 and CO_2. Dotted graph displays a blank Cr-Au electrode, which was measured under the same conditions for comparison.

The graph of the blank Cr-Au electrode in Figure 12 revealed no oxidation or reduction peaks in the measured potential window. Upon increased reductive potential, an increased current density trend could be noted with an onset of - 850 mV, which could be described as the beginning of hydrogen evolution. A similar trend was seen for the investigation of the PTCDA/Cr-Au electrode. Additionally, many reductive peaks (- 469 mV, - 892 mV) and oxidative peaks (- 631 mV, - 532 mV, -184 mV, and 42 mV) were found with PTCDA under N_2. It was not found that peaks were absent or decreased under CO_2 conditions, which would indicate an uptake or desired capture of CO_2 molecules.[36] However, it was seen that locations and intensities of the oxidation peaks remained the same upon comparison under N_2 nevertheless, the before observed single reduction peak at - 469 mV was separated into two peaks (- 469 mV and - 560 mV) and the second reduction peak at - 892 mV was shifted towards higher reductive potential (- 955 mV) under CO_2. In order to suppress the hydrogen evolution during the measurements and prevent the reaction of gold with CO_2, a more suitable substrate like glassy carbon (GCE) was used for further experiments. The CV graph of PTCDA/GCE can be seen in Figure 13.

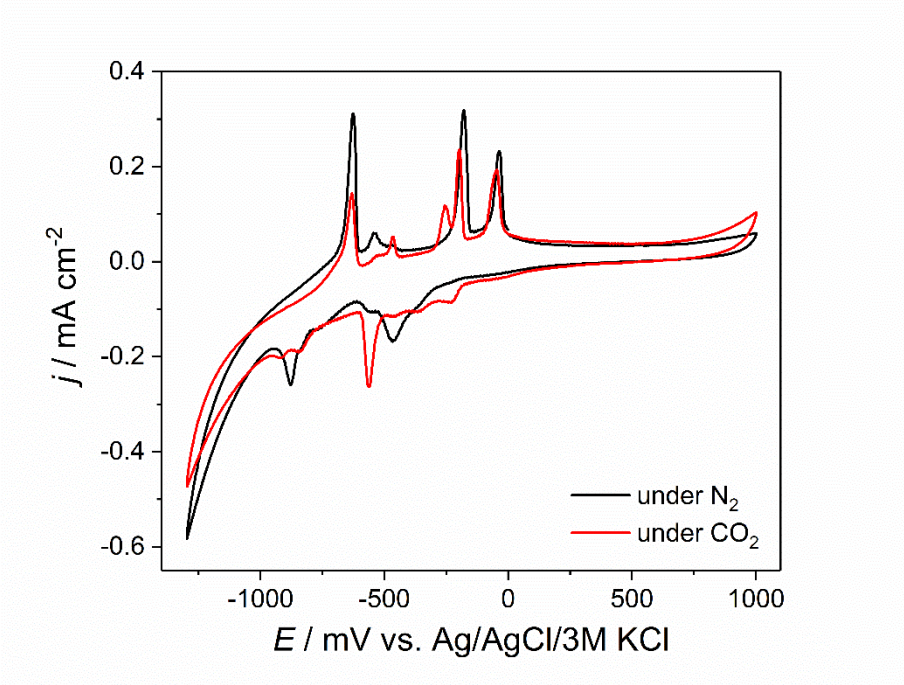

Figure 13: PTCDA on GCE in 0.1 M phosphate buffer (pH 7) under N_2 and CO_2.

In contrast to Figure 12, the now visibly better separated and higher in intensity oxidation and reduction peaks (Figure 13) were the result of the change of substrate, which suppressed the hydrogen evolution at high reductive potentials as seen from the low current density at - 1300 mV compared to Figure 12. It was noted that reduction and oxidation of the material both occurred under N_2 and CO_2 conditions, which confirmed that CO_2 is not being electrochemically captured, similarly as observed before. The slightly decreased current density towards high reductive potentials under CO_2 conditions, compared to the graph under N_2, was thereby not an effect of CO_2 capturing but was solely originating from the utilized glassy carbon electrode, which showed similar behavior during blank measurements. The CV graph under CO_2 however displayed different behavior compared under N_2, such as peak splitting and shifting, which might be an indication that the material is undergoing structural changes under these conditions.

3.1.2. H_2PTCDI

Similar to PTCDA, H_2PTCDI shares the same perylene backbone and the two dicarboxylic-dianhydride groups, however the two oxygen atoms are substituted with nitrogen atoms, which is then referred to as a bisimide and can be seen in Figure 14. A structure with an carbonyl-group, like anthraquinone, has already shown great results for CO_2 capturing and storing [75], which suggests promising properties for H_2PTCDI. The powder of the material has a black color and the chemical structure of H_2PTCDI can be seen in Figure 14.

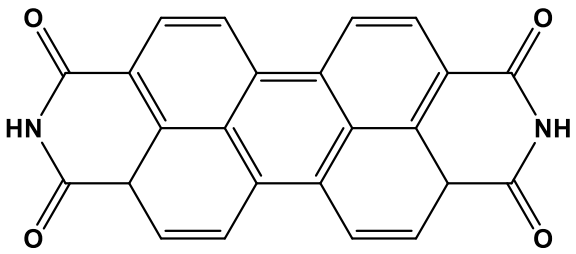

Figure 14: Chemical structure of H_2PTCDI.

First, a H_2PTCDI/Cr-Au electrode was electrochemically tested, similar to PTCDA, in organic electrolyte, which can be seen in Figure 15.

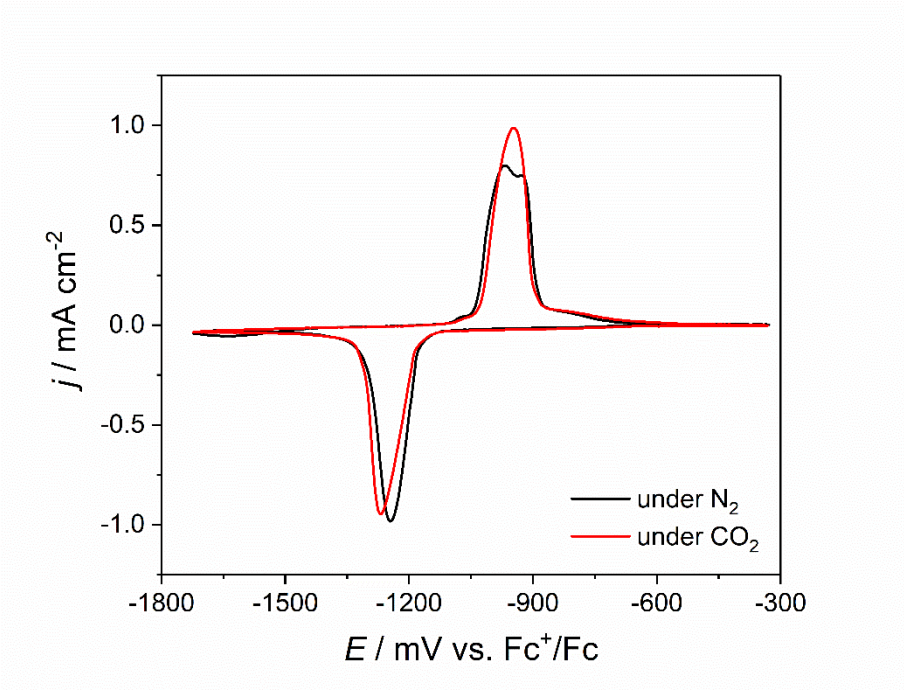

Figure 15: H_2PTCDI on Cr-Au in 0.1 M $TBAPF_6$ / MeCN under N_2 and CO_2.

The CV of the electrochemical behavior of H_2PTCDI in Figure 15, shows a single reduction and oxidation peak. It was noticed that the oxidation peak under N_2 was slightly separated by a peak maxima difference of 40 mV.

Figure 16 displays the CV of a H_2PTCDI/GCE in 0.1 M phosphate buffer (pH 7), which showed none of the above-mentioned disadvantages of these systems.

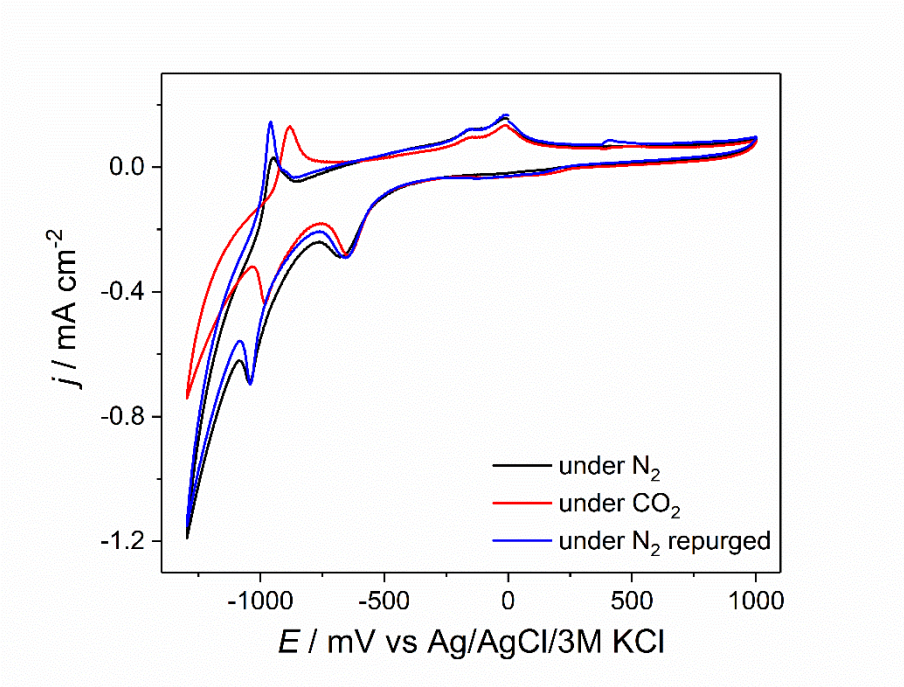

Figure 16: H_2PTCDI on GCE in 0.1 M phosphate buffer (pH 7) under N_2 and CO_2.

The same experimental conditions were applied in Figure 16 as displayed in Figure 13. The cell with the H_2PTCDI electrode was repurged for one hour with nitrogen after the measurements under N_2 and CO_2 to reveal that the material showed the same electrochemical behavior equally to the first investigation under N_2. This was observed by the same peak positions and similar peak intensities for reduction and oxidation for both N_2 CV plots. Nevertheless, an interesting behavior was found upon measuring the material under CO_2 conditions, since the peak position of the highest reductive and lowest oxidative potential were both shifted towards higher oxidative potential, which was not observed for other peaks. This observed behavior might be due to a change in kinetic under carbon dioxide purged conditions. In this case, a reaction of the material towards effective CO_2 capturing properties was not observed again, since both reduction and oxidation peaks were still occurring with little to no change in peak intensity.

3.1.3. Diphy-PTCDI

Diphy-PTCDI can be synthesized from PTCDA [74] and has one phenyl group attached to each nitrogen atom of the bisimides, which are now tertiary amines through the replacement of the two hydrogen atoms. As previously mentioned, materials of this class with improved functionalized groups were utilized by Apaydin *et al.*[36] for CO_2 capture experiments. The chemical structure for diphy-PTCDI, which has a brown color, can be seen in Figure 17.

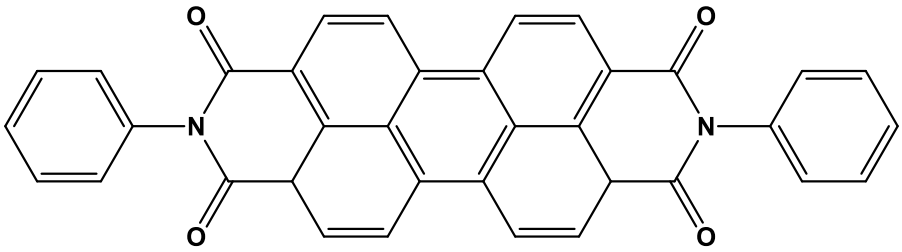

Figure 17: Chemical structure of diphy-PTCDI.

A Diphy-PTCDI/Cr-Au electrode was measured first in organic electrolyte. The resulting CV can be seen in Figure 18.

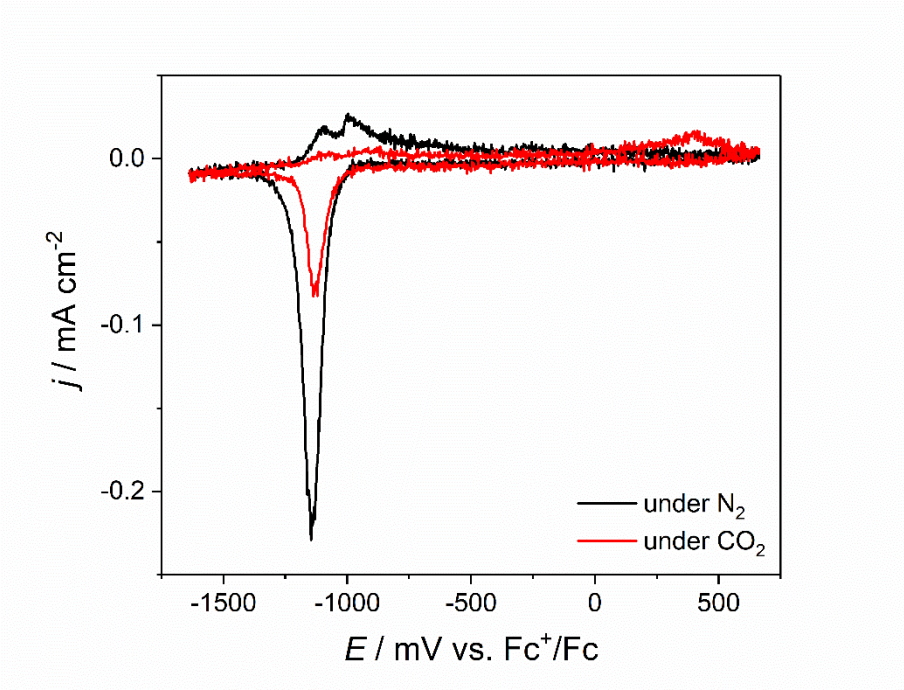

Figure 18: Diphy-PTCDI on Cr-Au in 0.1 M $TBAPF_6$ / MeCN under N_2 and CO_2.

Similar to the before investigated perylene derivatives, a severe stability issue of the film was observed during the electrochemical measurement of diphy-PTCDI in the organic electrolyte. This issue was noted as the film material started to dissolve into the electrolyte solution around the reduction peak at - 1147 mV. Therefore, the seen decreased current density in Figure 18 under CO_2 was suggested to be the result of the instable film under both N_2 and CO_2 conditions.
Furthermore, a diphy-PTCDI/GCE electrode was electrochemically measured in 0.1 M phosphate buffer (pH 7), which resulting CV is depicted in Figure 19.

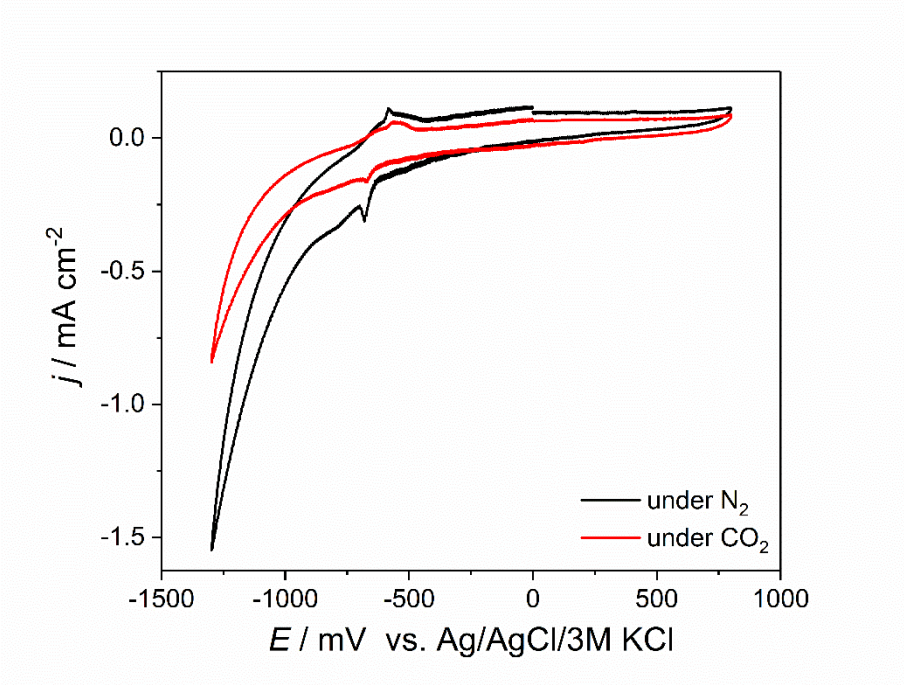

Figure 19: Diphy-PTCDI on GCE in 0.1 M phosphate buffer (pH 7) under N_2 and CO_2.

Figure 19 shows two graphs under N_2 and CO_2 with the same reductive peak at position - 684 mV and an oxidative peak at - 588 mV, for the 100 nm diphy-PTCDI film on a glassy carbon electrode. The overall current density for the CO_2 plot was noticeably smaller than the current density of the N_2 plot. However, this effect could not be interpreted as a behavior towards CO_2 capture, since the same stability issues also occurred in the utilized buffered electrolyte system and a loss of material (dissolving) was observed. Therefore, diphy-PTCDI turned out to be the least stable material in all three investigated electrolyte solutions, compared to the previously measured perylene derivatives.

3.1.4. PANI as mediator together with perylene derivatives

The following subchapter is about the addition or incorporation of aniline or polyaniline respectively, into the aforementioned perylene derivatives. Therefore, electrodes with a bilayer arrangement or an in-situ electropolymerized film of both materials were developed and tested, whereas most of the utilized substrates involved Cr-Au electrodes and glassy carbon electrodes only to a certain extent.

3.1.4.1. H_2PTCDI/PANI bilayer arrangement

An electrode with a 100 nm film of H_2PTCDI on Cr-Au and an additional top layer of polyaniline was produced to study possible enhancements towards CO_2 capture/reduction. Polyaniline was hereby chosen as capable polymer to reduce CO_2, which was previously studied by Hursán *et al.*[27]. The unconventional layout of PANI on top of H_2PTCDI was chosen, since the

electropolymerization of a PANI film as first layer resulted in a rough film with various pores, which would pose an unacceptable foundation for a desired uniform thin film, such as H_2PTCDI. On the other hand, another possible drawback was taken into account with the polymerization of PANI on top of H_2PTCDI, since it was done in very acidic solution, which might have altered the surface properties of the thin film. Therefore, a PANI film was electropolymerized onto a H_2PTCDI/Cr-Au electrode and electrochemically characterized. The CV of the PANI/H_2PTCDI/Cr-Au electrode in 0.1 M phosphate buffer (pH 7) is depicted in Figure 19.

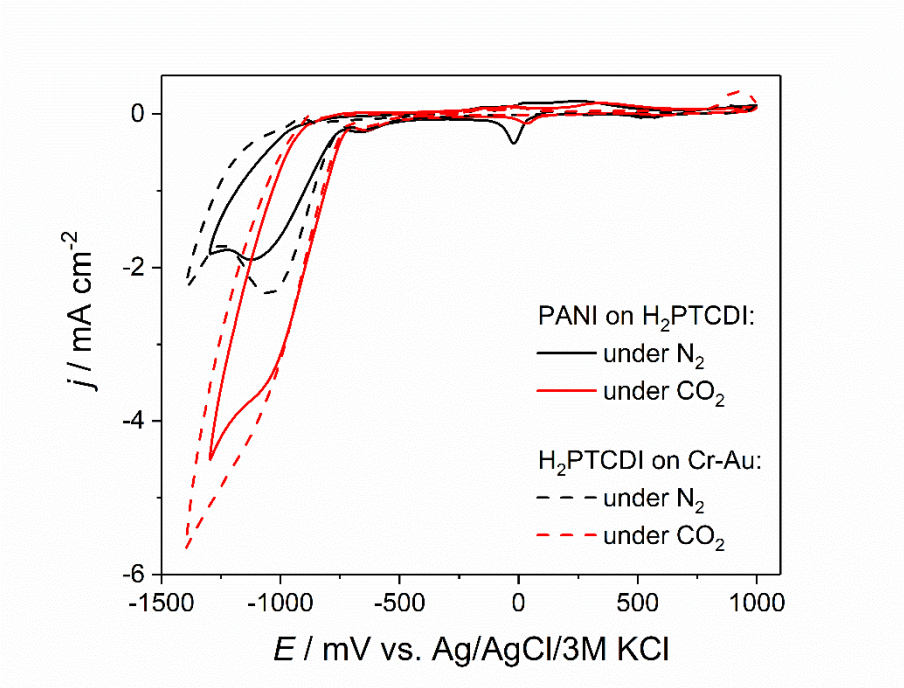

Figure 20: PANI on H_2PTCDI on Cr-Au in 0.1 M phosphate buffer (pH7) under N_2 and CO_2. Dotted line shows a reference CV of H_2PTCDI on Cr-Au, measured under the same conditions. Polymerization was conducted in 1 M H_2SO_4 with 25 mM aniline electrochemically from +800 mV to -150 mV vs. Ag/AgCl at 25 mV s^{-1} for 10 cycles.

The CV of the bilayer electrode in Figure 20 shows no major deviations from the depicted reference sample. However, the addition of PANI revealed a further reduction peak at - 22 mV for N_2 and 34 mV for CO_2. Nevertheless, the conducted measurements on the bilayer electrode had proven to be rather difficult after purging the system with CO_2, which resulted multiple times in an exfoliation of the whole active film. This recurring effect might be due to the previously discussed fact that the electropolymerization of aniline was conducted in acidic media, which might have altered the surface properties of the H_2PTCDI film. Therefore, further structural changes during the polymerization couldn't be excluded, which possibly imposed additional stability issues to the active film layer.

Furthermore, the characteristic oxidation and reduction peaks of polyaniline, which can be seen in the next subchapter in Figure 22, are not visible in Figure 20. One of the main reasons for this effect are the very different pH values of the utilized electrolyte solutions (pH 7 vs. pH 0) that

influenced the electrochemical characteristics of the polymer, since it is known that PANI is more conductive when polymerized under lower pH values. In addition, the distinct substrates and electropolymerization parameters that were used in those experiments differ from each other. Moreover, the thin PANI film in Figure 20 was electropolymerized directly onto the H_2PTCDI/Cr-Au film under very acidic conditions that induced stability issues as previously mention, whereas the electropolymerization in Figure 22 was done in direct contact with a pristine glassy carbon electrode with PTCDA in the electrolyte solution.

3.1.4.2. Electro-co-polymerization of PTCDA and H_2PTCDI with aniline

The electro-co-polymerization of a perylene derivative and polyaniline posed to be a difficult endeavor. As a consequence, both materials would have to be dissolved into the utilized electrolyte solution, which minimized the choices of a sufficient solvent, since the perylenes were sparingly soluble. The resulting mixtures of commercially available PTCDA and aniline in various solutions can be seen in Figure 21.

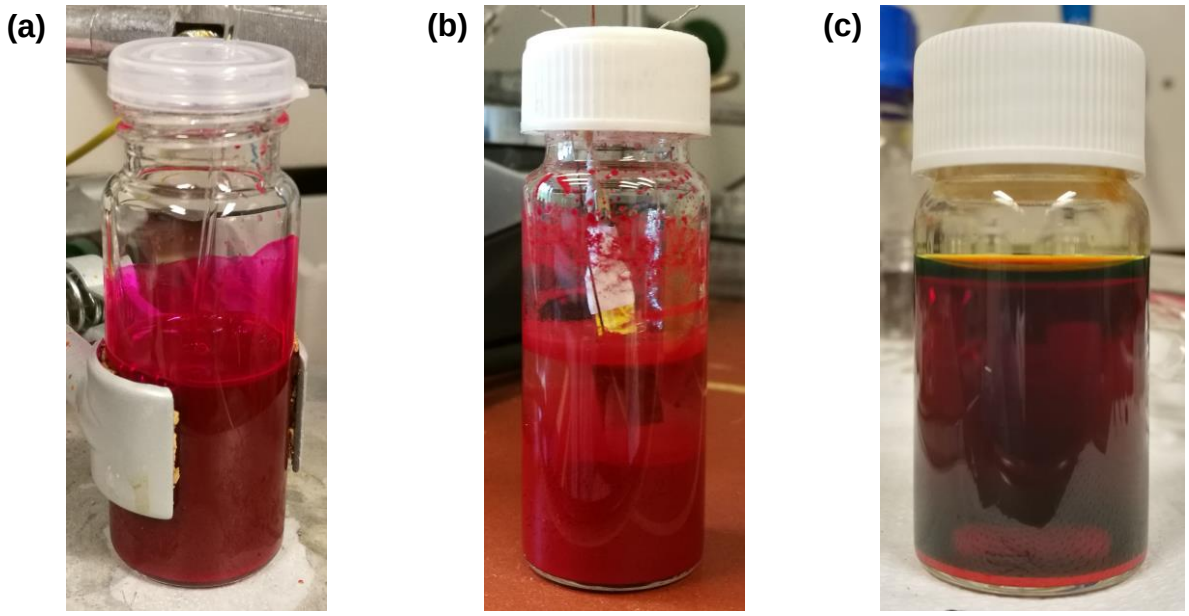

Figure 21: Mixture of PTCDA and aniline in different solutions like (a) conc. H_2SO_4, (b) 1 M H_2SO_4, and (c) 0.1 M KOH.

A primary approach was to dissolve both materials in concentrated sulfuric acid, whereas the perylene would be dissolved first and then an equimolar amount of aniline would be added. Although the PTCDA dissolved very nicely, as seen in Figure 21 (a), a sizzling sound and fog evolution was perceived upon the addition of aniline to the solution. According to literature [76], the nitrogen atom of aniline gets protonated under very acidic conditions, which leads to an addition of the sulfonate group to the para position of the aromatic ring and produces therefore the sulfanilic acid, which is unable to be further polymerized to PANI.

Another Approach was to utilize a 1 M H_2SO_4 electrolyte, since the polymerization of aniline was usually conducted in it. As depicted in Figure 21 (b), the PTCDA would not dissolve in this solvent and would usually accumulate at the bottom of the vessel. However, an attempt was made to electro-co-polymerize PTCDA and aniline and the resulting CV scan is shown in Figure 22.

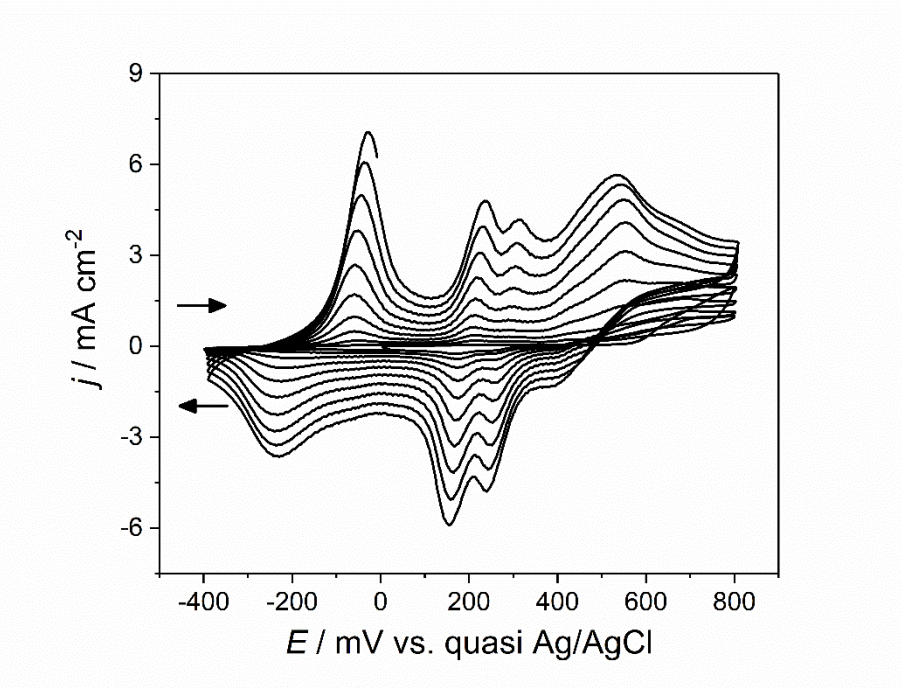

Figure 22: Electro-co-polymerization of PTCDA and aniline (*n*:*n* = 1:1) on GCE in 1 M H_2SO_4 electrolyte. 25 mM aniline with 25 mV s^{-1} for 10 cycles after 1 hour purging with N_2.

Going from negative to positive potential during the oxidation in Figure 22, multiple peaks an - 28 mV, 235 mV, 312 mV and 532 mV were observed, which were subsequently reduced, going from positive to negative potential at 395 mV, 240 mV, 155 mV, and - 230 mV. The CV with its characteristic peaks resembled the electropolymerization of aniline in alinement with Morávková *et al*.[77], since the first oxidation peak (- 28 mV) could be assigned to the leucoemeraldine species of PANI and the last oxidation peak (532 mV) showed the formation of the pernigraniline. The oxidation peak in the middle usually shows the formation of hydroquinone-like defects [77]. However, in this case two oxidation peaks were observed, which could be due to the addition of PTCDA or the utilized Cr-Au substrate.

The produced film resembled primarily to a thick film of polyaniline, due to its roughness and green color. Nevertheless, small red spots were visible with bare eyes, which sparked further investigations of the film surface under a microscope and scanning electron microscopy (SEM). The corresponding pictures can be seen in Figure 23.

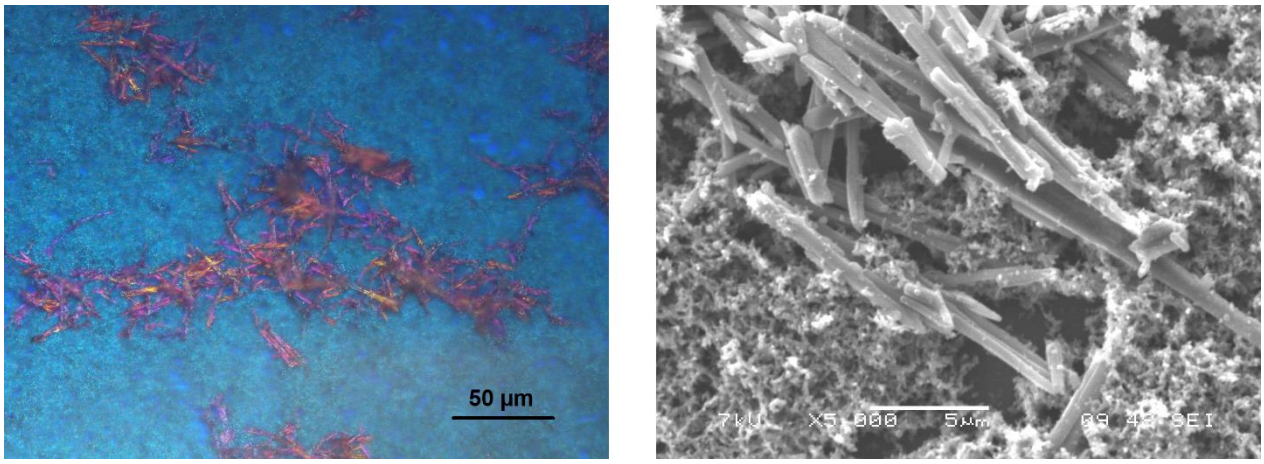

Figure 23: Surface images of the PTCDA/PANI/GCE electrode under a light microscope (left) and SEM (right).

The microscopic images in Figure 23 show that needles of PTCDA had been successfully incorporated into the framework of PANI. It is suggested that PTCDA agglomerated onto the surface and partially into the electropolymerized polyaniline mesh. The SEM picture on the right sight gives am improved insight into the incorporation of the PTCDA needles, whereas some are embedded, some are slightly covered, and few are stuck on top of each other.

Nevertheless, the electrode with the described film could not be electrochemically characterized in 0.1 M phosphate buffer (pH 7), since the resistivity of this material composition was too high. It was suggested from the observed behavior that the combination of materials might form a less conductive film than polyaniline itself. In addition to that, a polymerization between the two materials could not be optically proven, since the appearance of the film showed a pure phase of PANI and PTCDA needles as another phase. An identical behavior was observed as well for the combination of H_2PTCDI and PANI on a Cr-Au electrode. The corresponding microscopy images are depicted in Figure 24.

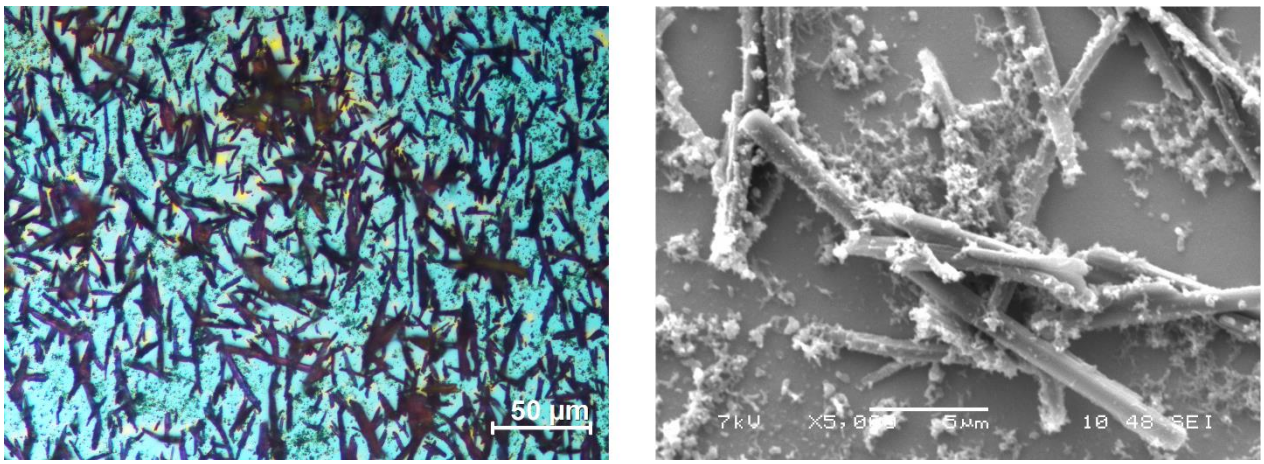

Figure 24: Surface images of the H_2PTCDI/PANI/Cr-Au electrode under a light microscope (left) and SEM (right).

Therefore, further emphasis was taken towards the electro-co-polymerization of PTCDA and H_2PTCDI with aniline in basic electrolyte solution, such as 0.1 M KOH. Concentrations of the involved materials were kept identical; however, the electropolymerization procedure had to be changed due to the change of the pH and therefore the potential. A standardized procedure with a fixed potential range was determined throughout extensive testing with Cr-Au electrodes. It was found that a pre-polymerization ranging from 800 mV to - 1000 mV vs. Ag/AgCl for 3 cycles, followed by the primary polymerization for 20 cycles between 800 mV to - 1500 mV vs. Ag/AgCl at 25 mV s^{-1} in the same solution, enabled the best results in terms of film formation and reproducibility of the experiments. The produced films of both material compositions on Cr-Au and glassy carbon electrodes are shown in Figure 25.

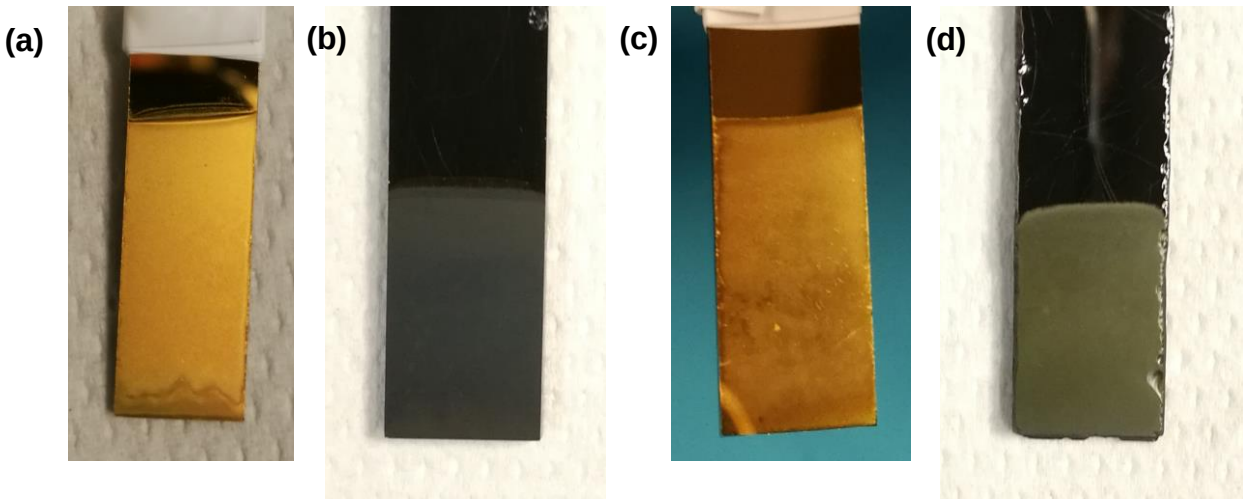

Figure 25: Electro-co-polymerized film of PTCDA/PANI from 0.1 M KOH on (a) Cr-Au and (b) glassy carbon, and film of H_2PTCDI/PANI from 0.1 M KOH on (c) Cr-Au and (d) glassy carbon.

The CV behavior during the electro-co-polymerization of PTCDA and PANI was studied with various blank experiments. Hereby, polymerization experiments were made with only PTCDA and PANI on Cr-Au in 0.1 M KOH to observe a change in behavior. The corresponding combined CV of all measurements is presented in Figure 26.

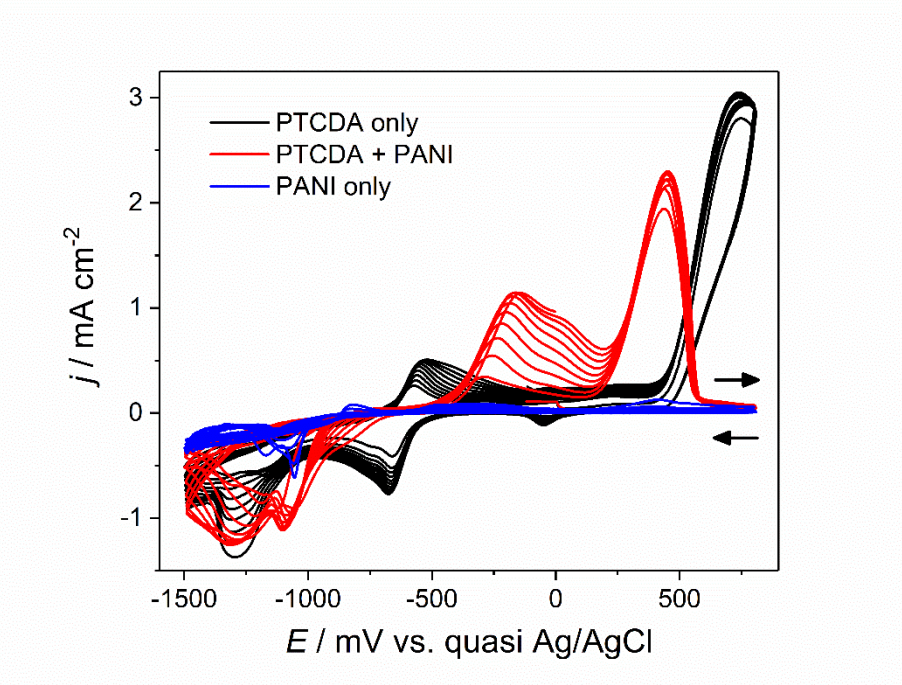

Figure 26: Electro-co-polymerization of PTCDA with aniline in 0.1 M KOH on Cr-Au with reference CVs, such as only PTCDA and only PANI for comparison.

The CV plot where only PANI was electropolymerized in Figure 26, showed clearly a decreased activity upon comparison with the other materials. This suggests that the formed PANI was relatively in-active and demonstrates that it was only polymerized in small and probably less-conductive quantities because of the high alkaline 0.1 M KOH (pH = 13) solution.[78]
The PTCDA graph on the other hand, showed already two major reduction peaks at - 675 mV and - 1295 mV and two oxidation peaks at - 521 mV and 740 mV, which increased with every count of cycles. The addition of both materials however, revealed also an increase of the peak intensities with increased number of cycles on Cr-Au but also a shift of the reduction (- 1100 mV, - 1318 mV) and oxidation (- 159 mV, 450 mV) peaks. The formed film is depicted in Figure 25 (a). Throughout these results, another polymerization of PTCDA and aniline was conducted on a glassy carbon electrode and the obtained film (Figure 25 (b)) was electrochemically characterized in 0.1 M phosphate buffer (pH 7), which can be seen in Figure 27.

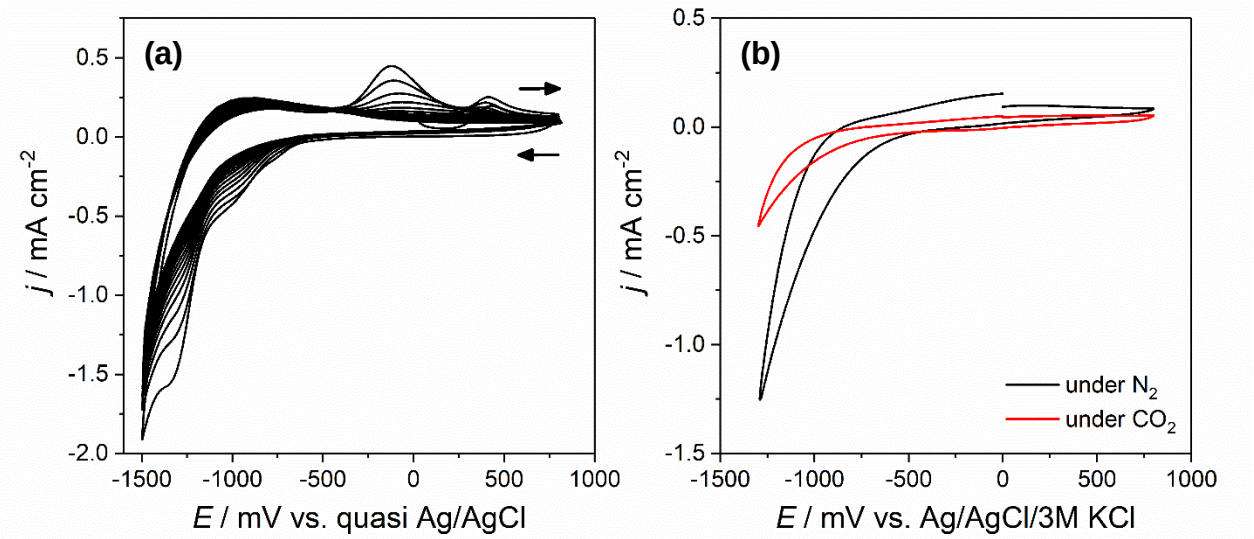

Figure 27: (a) Electro-co-polymerization CV of PTCDA and aniline in 0.1 M KOH onto GCE. (b) CV of PTCDA/PANI/GCE film from 0.1 m KOH in 0.1 M phosphate buffer (pH 7) under N_2 and CO_2.

Contrary to the previously observed behavior of PTCDA and PANI on Cr- Au in Figure 26, the CV for the electro-co-polymerization on GCE in Figure 27 (a) depicts different positions for its reduction and oxidation peaks, as well as different peak intensities. It was also observed that the current density was decreasing with increased number of cycles. While this change might have had occurred because of the different usage of substrate material, it had significant effects on the film growth, since only a slightly grayish film was observed after the polymerization. The electrochemical characterization of the obtained film on GCE (Figure 25 (b)) showed no characteristics nor similarities of the evaporated PTCDA film.

The characteristics of H_2PTCDI were tested under the exact same conditions, to determine whether a similar behavior to PTCDA would be observed or a way to produce a film with an electrochemical behavior of H_2PTCDI could be found. Figure 28 shows similar to PTCDA the electro-co-polymerization behavior of H_2PTCDI and aniline in 0.1 M KOH, as well as the electrochemical behavior of the obtained film in 0.1 M phosphate buffer (pH 7).

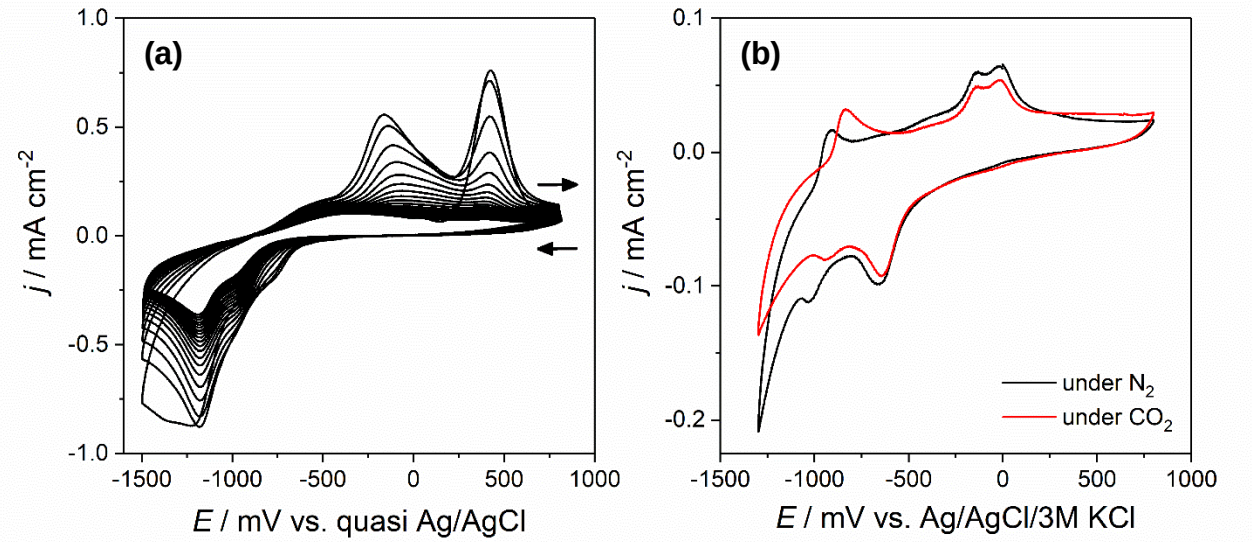

Figure 28: (a) Electro-co-polymerization CV of H_2PTCDI and aniline in 0.1 M KOH onto GCE. (b) CV of H_2PTCDI /PANI/GCE film from 0.1 m KOH in 0.1 M phosphate buffer (pH 7) under N_2 and CO_2.

As depicted in Figure 28 (a) the electro-co-polymerization shows a major reduction peak at - 1183 mV and two oxidation peaks at - 166 mV and 424 mV. In accordance with the observed polymerization behavior of PTCDA, the current density was decreasing with increased number of cycles for H_2PTCDI as well. However, the electrochemical measurement of the received greenish film (Figure 25 (d)), in Figure 28 (b) showed a similar behavior to the previously measured evaporated H_2PTCDI film on GCE (Figure 16). This result suggests that it is possible to electrochemically cast a H_2PTCDI film onto a substrate from a material loaded 0.1 M KOH solution.

The observed quality of film formation with H_2PTCDI was not found while using PTCDA, which sparked further emphasize towards the possible film formation of PTCDA under improved conditions. It was observed that the solution of KOH became dark red, while the solution on the top showed a green yellowish color. The solution showed luminescent characteristics upon illumination of the vessel with a UV-lamp, which revealed that another fluorescent species must had been formed while PTCDA was exposed to the KOH solution. The solution was diluted 1:100 with MQ water, transferred to a quartz cuvette, and the absorption and fluorescence were measured. The now described stages of the investigation of PTCDA in 0.1 M KOH solution can be seen in Figure 29, starting with its color upon immediate insertion into the basic solution. The graph of the absorption and fluorescence of the diluted sample (Figure 29 (d)) is depicted in Figure 30.

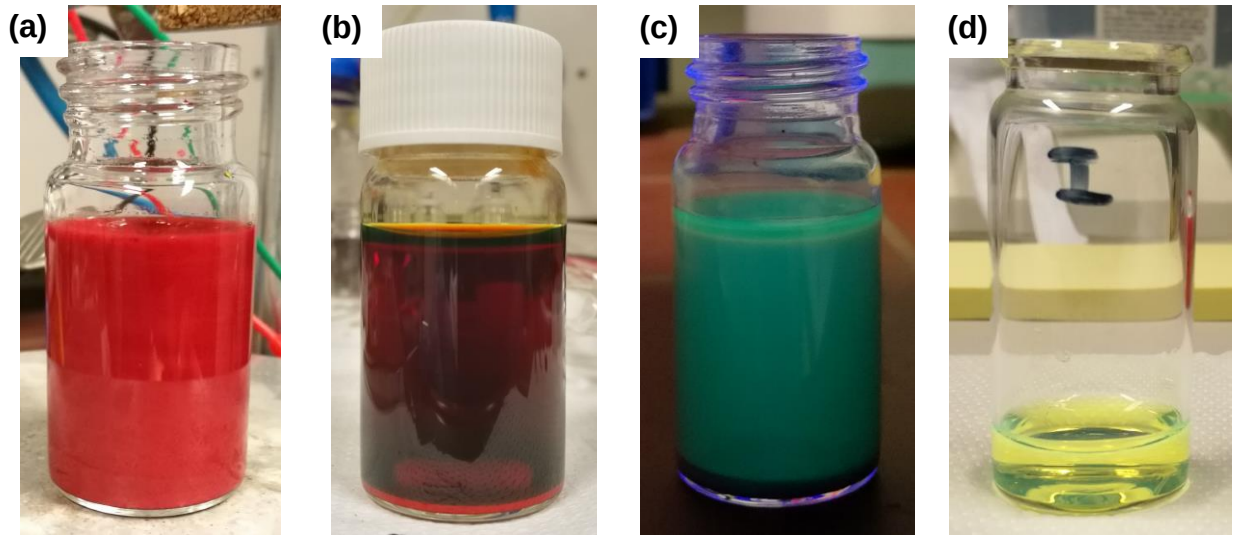

Figure 29: Stages of PTCDA in 0.1 M KOH solution (a) upon immediate mixing, (b) after 1 hour, (c) upon illumination with an UV-lamp, and (d) after dilution (1:100) with MQ water.

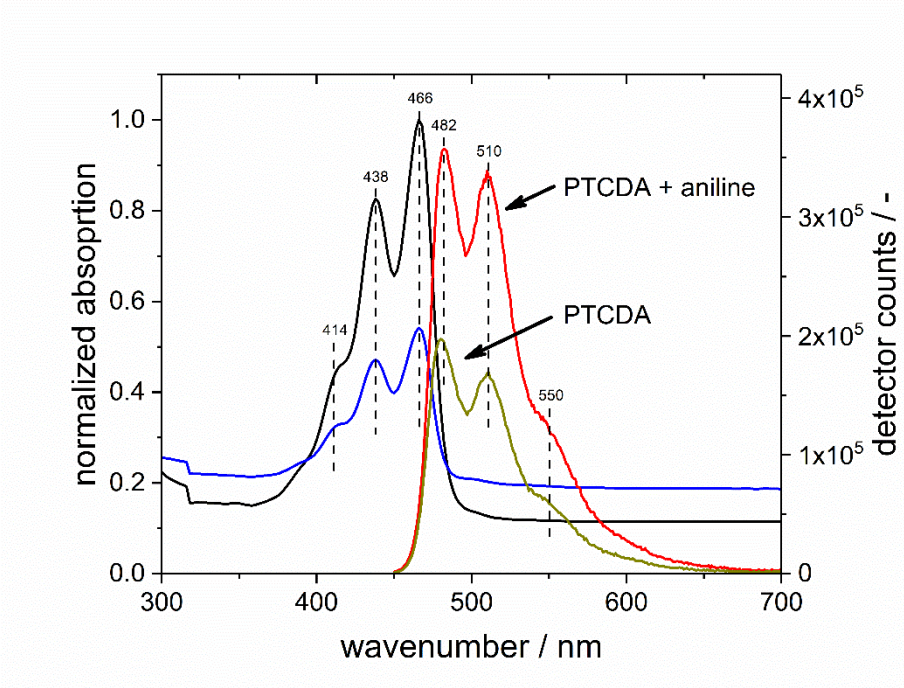

Figure 30: Absorption and emission spectra of diluted (1:100) PTCDA and PTCDA + PANI solutions from 0.1 M KOH.

The graph in Figure 30 shows that the addition of aniline to the PTCDA solution does not affect the position of the absorption of emission peaks; however, a decrease in intensity was noted, which likely arose from a deviation of the dilution factor. Observed were three absorption peaks at 414, 438, and 466 nm and three corresponding emission peaks at 482, 510, and 550 nm. According to Langhals *et al*. [79] these absorption and emission peaks correspond to the perylene tetracarboxylic acid, which revealed that both rings of the dianhydride of PTCDA opened up in the 0.1 M KOH solution throughout a nucleophilic attack of the surrounding OH anions on either of both carbonyl groups in the ring, which formed a tetracarboxylic anion species. Upon dilution in

neutral MQ water the species regains four protons, which is the reason why the perylene tetracarboxylic acid was identified.

This fact suggested that the soluble species of PTCDA in solution was the previously observed species mentioned above. Nevertheless, this also indicated that the amount of PTCDA being dissolved in solution might be dependent on the reaction time between the material and KOH. Usually, all conducted polymerization experiments were finished within 90 minutes after the material was added to the solution. In order to raise the amount of dissolved PTCDA, another experiment was conducted where the material was exposed to the KOH solution for a duration of 4 days, whereas one day was used for stirring the solution and the remaining days allowed the non-dissolved PTCDA to accumulate at the bottom of the reaction vessel. Afterwards, an electropolymerzation in this solution was conducted on a Cr-Au electrode and it was found that indeed a red film of PTCDA was formed on top of the electrode. Throughout additional characterization with FTIR and comparison of the results with literature [80],it was found that PTCDA was formed as a film on top of the Cr-Au, which can be seen in Figure 31.

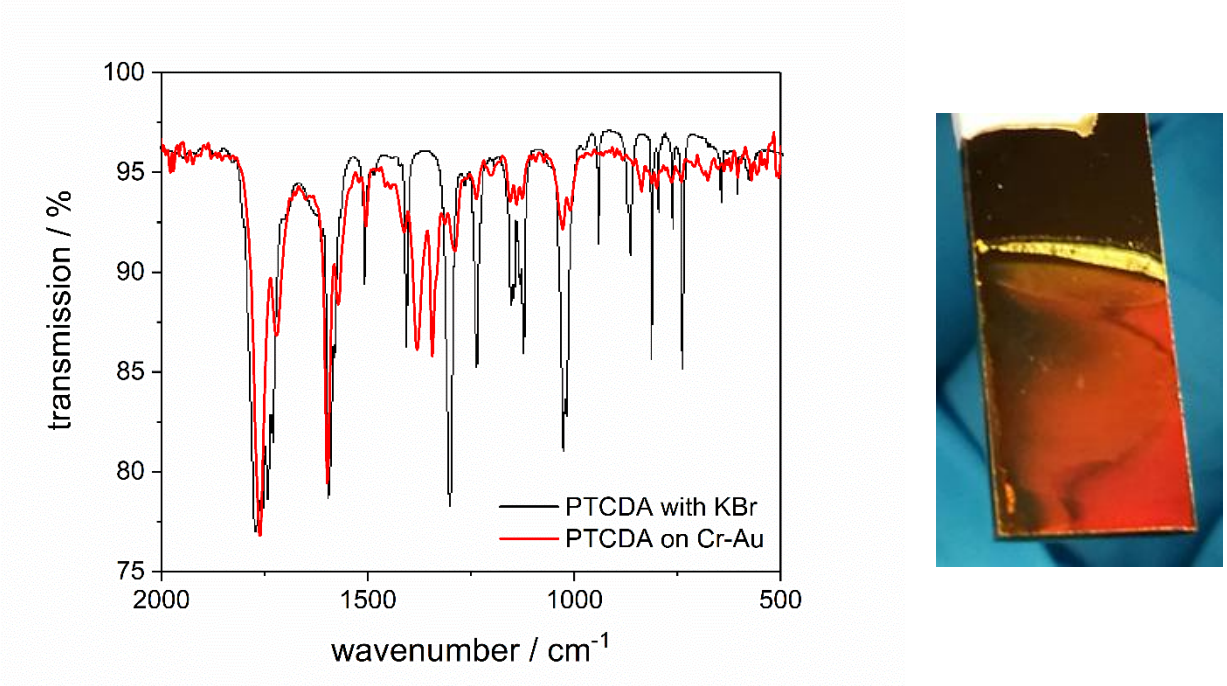

Figure 31: FTIR spectrum of electropolymerized PTCDA on Cr-Au film (red) and the FTIR spectrum of the literature reference [80] (black) (left). Image of the processed film of PTCDA on Cr-Au (right).

The portrayed FTIR spectrum in Figure 31 shows that the observed vibrational peaks of the sample and the reference were in fact the same. The most noticeable and important vibrational bands can be seen at 1760 and 1730 cm^{-1}, which are assigned to carboxylic group with a dianhydride character.[81],[82] However, small deviations were noticed for the sample between 1300 and 1400 cm^{-1}, which could be addressed by mentioning that the utilized electrode perhaps contained some minor impurities and the transmission of the Cr-Au underneath the film was also

measured. Nevertheless, the claim that the Cr-Au material under the film interfered with the previously mentioned characteristic peaks for PTCDA were excluded by plotting the differential infrared spectrum, whereby the IR vibrations of the substrate material were excluded and the characteristic vibrational bands at 1760 and 1730 cm^{-1} were still visible.

3.2. Carbon utilization properties

This chapter is about the demonstration of the CO_2 reduction properties of solely electropolymerized polyaniline throughout photoelectrochemical experiments. The main focus hereby lies in the reproduction of the results of Hursán *et al.*[27] who used said polymer to photoelectrochemically reduce CO_2 to alcohols. Furthermore, additional steps were taken to optimize the procedure and to investigate the properties of polyaniline towards carbon monoxide evolution.

3.2.1. Polyaniline as active material for alcohol products

Polyaniline has been known for many decades and has been investigated for numerous applications such as paint coatings, electrodes in batteries, and framework material for metal catalysts.[67],[70] It has been proven that polyaniline, in combination with co-catalysts such as metals (e.g. copper), show electrochemical reactions towards methanol and ethanol production [30]. However, the previously named research group [27] showed that solely polyaniline could be utilized to favor photoelectrochemical methanol and ethanol production in aqueous media. Therefore, the experimental conditions were adapted and retained to re-enact the experimental procedure for comparable results.

The utilized setup, consisting of the electrochemical H-cell and a lamp setup, which was used for the following results was already described in point 2.4.5. Firstly, freshly distilled aniline was potentiodynamically electropolymerized in 0.5 M H_2SO_4 onto GCE with a total charge density of 245 mC cm^{-2} instead of the 150 mC cm^{-2}, which was mentioned in the paper. This was achieved by running the electropolymerization for a minimum of 5 cycles, which was a necessity for further usage to obtain a homogeneous and thick enough film, whereas the excess of charge density was received from the last cycle that contributed with 90 mC cm^{-2}. The PANI electrode was then placed into the H-cell, which was filled with 120 mL of 0.1 M Na_2SO_4 electrolyte. The cell was purged for 1 hour with N_2 and 1 hour with CO_2, whereas after each purging cycle a CV and chronoamperometric measurement (under dark and illumination) was conducted. Then the cell was completely sealed with nail polish and a photoelectrolysis was conducted for 2 hours under CO_2 at – 0.4 V vs. an Ag/AgCl/3M KCl reference electrode under illumination (80 mW cm^{-2}). Afterwards, the gas in the head space was analyzed with GC and the electrolyte was analyzed

with liquid injection GC and IC.

It was found that mostly hydrogen evolved (15% faradaic efficiency) during the photoelectrolysis, whereas no traces of methanol or ethanol were detected. Hursan *et al.*[27] reported, a 20% FE for H_2 evolution, ~43% FE for methanol and ~ 20% FE for ethanol (2:1 ratio). In addition, the reported current density increase upon illumination of the PANI electrode under CO_2 was found to be not in the range of 20-70 µA cm^{-2} but more in 3-5 µA cm^{-2} at - 0.4 V, as depicted in Figure 32.

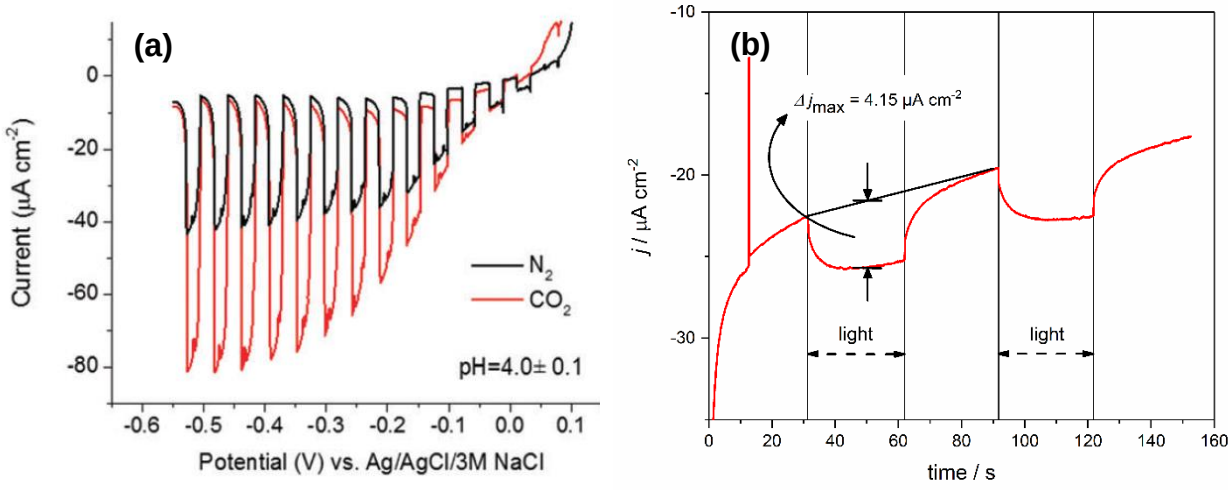

Figure 32: (a) Photovoltammogram from Hursán *et al.*[27] of an electrodeposited PANI layer under chopped UV-Vis illumination (Xe-Hg arc lamp, 100 W output) in N_2- and CO_2-saturated 0.1 M Na_2SO_4 aqueous solution where the N_2-saturated solution was buffered to pH = 4.0. (b) Chronoamperometry of PANI on GCE in 0.1 M Na_2SO_4 electrolyte at - 0.4 V under CO_2 (red line) and under alternating 30 seconds dark and 30 seconds illuminated (80 mW cm^{-2}) conditions.

The group reported a photovoltammogram (Figure 32 (a)) that shows the behavior of a PANI film over multiple voltages with and without illumination. The interesting behavior of the material took place during the electrolysis where - 0.4 V were applied, which is why a chronoamperometric measurement, like in Figure 32 (b) was preferred over the reported method. Although smaller experimental errors could not be excluded, it seemed highly unlikely that 5-20 times higher current density could be achieved, using the same conditions. Another point is that a certain redox potential must be applied in order to overcome the needed Gibbs free energy and to enable the conversion of CO_2 to methanol. According to literature [16],[17] a minimum potential of -0.38 V vs. NHE at pH 7 has to be applied for a successful conversion from carbon dioxide to methanol, without taking into account that a certain overpotential of additional - 0.2 V would be practically needed. This equals 64 mV vs. RHE (reversible hydrogen electrode) at pH 4.3, which would require at least a potential of - 0.59 V vs. Ag/AgCl/3M KCl at pH 4.3. This shows that the utilized - 0.4 V potential for electrolysis was too low by itself. However, the gap in the required thermodynamical potential was presumably closed by the additional introduction of photons through illumination of the electrode. A total amount of three repetitive experiments suggested that the formation of alcohols was not possible under the proposed conditions. The proposed results and the identical experimental conditions prove that the results of Hursán *et al*. are incorrect or incomplete.

3.2.2. Polyaniline as active material for carbon monoxide evolution

From this point on, an attempt was made to improve the experimental conditions starting with the utilized electrolyte. Throughout the known literature [30] that used polyaniline as a framework material with incorporated metal catalysts to reduce CO_2 to alcohols, it was stated that factors like temperature, pH range, and amount of dissolved CO_2 in the electrolyte solution make an essential impact on the amount of product formation. Multiple research groups utilized methanol as a CO_2 rich solution with small mM amounts of sulfuric acid.[24],[30] However, they were interested in the formation of alcholos. A commonly used electrolyte in this field is a 0.5 M potassium bicarbonate solution that can provide an increased concentration of dissolved CO_2 [83] and that changes its pH from 8.4 under N_2 to 7.3 under CO_2, which was the reason for implementing it into future experiments. Since Hursán *et al.*[27] also proved that their setup, with an output of 300 W, was capable of performing equally to their setup with 100 W, a more powerful illumination source (Xe-Hg lamp) was installed with a total output of 460 mW cm^{-2} for the following experiments. Nevertheless, the previously discussed issues with the inadequate utilization of a low potential had to be addressed as well, which was why the potential was increased to - 1.3 V vs. Ag/AgCl/3M KCl at pH 7.3. This was equivalent to - 0.66 V vs. RHE at pH 7.3, which has a theoretical overpotential of -0.56 V for carbon monoxide evolution at this certain pH. Another point that was observed was that the utilized PANI film seemed to be very thin and would turn colorless after the excessive exposure of the polymer to the illumination source. Therefore, the electropolymerization conditions were adjusted to receive a thicker and more uniformly grown polymer film. The procedure was described in point 2.3.3 as the utilized standard procedure and the resulting electropolymerization CV can be seen in Figure 33.

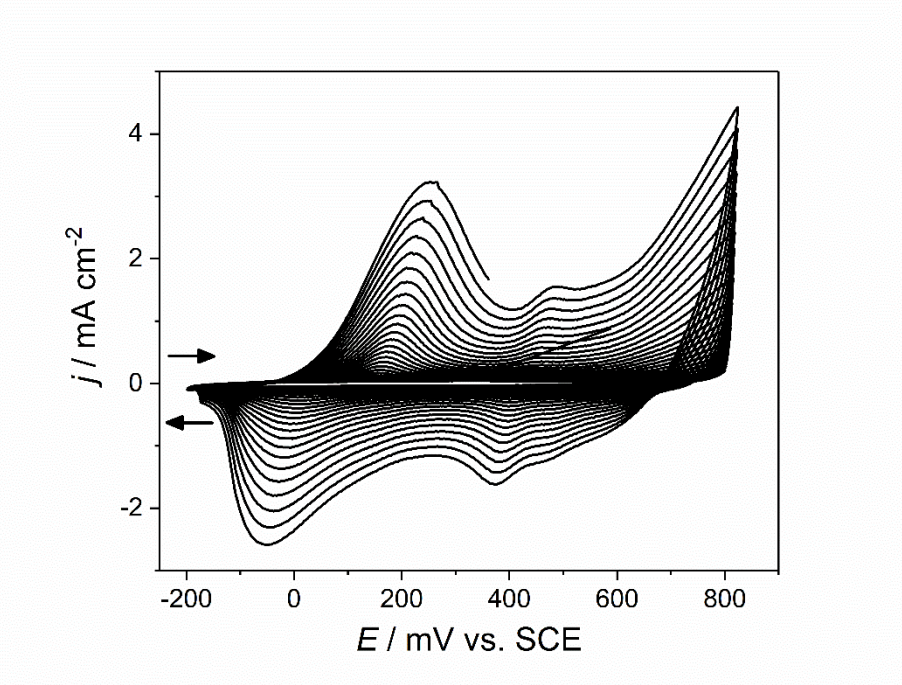

Figure 33: Electropolymerization of aniline in 0.5 M H_2SO_4 onto GCE. 0.1 M aniline with 25 mV s^{-1} scan rate for 25 cycles after 1 hour purging with N_2.

The CV in Figure 33 shows the electropolymerization of aniline in accordance with the literature [84],[85] ,whereas a saturated calomel electrode (SCE) was used as a reference electrode to cycle between 800 mV to - 200 mV. The peaks in this graph showed the different polyaniline species that occurred between the potentiodynamic polymerization, which were discussed before. However, in this case the electropolymerization cycles were completed at 350 mV in order to obtain the emeraldine salt, which is the most conductive form of polyaniline. The PANI electrode was then measured, similar to the previous experiments before but only with the stated modified conditions. The following Figure 34 (a) shows the behavior of the PANI-film in 0.5 M potassium bicarbonate under a reductive potential up to - 0.65 V vs. RHE and (b) the electrochemical behavior of the blank GCE under identical conditions.

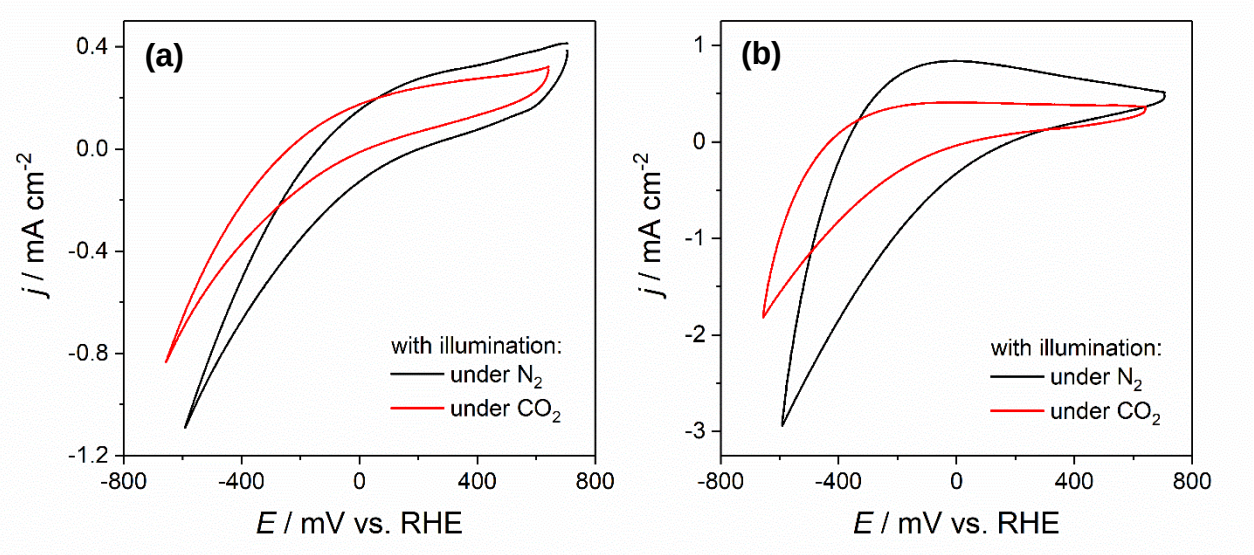

Figure 34: (a) CV of PANI on GCE in 0.5 M potassium bicarbonate electrolyte in reductive potential under N_2 and CO_2 and under illumination with 460 mW cm^{-2}. (b) CV of a blank GCE electrode measured under the same conditions.

The CV in Figure 334 (a) showed no specific reduction or oxidation peaks of PANI. One has to keep in mind that at such a high reductive potential, the only available species of PANI can be the leucoemeraldine, which has a reduced conductivity compared to the emeraldine salt. Furthermore, the current density at -0.65 V was higher under N_2 compared under CO_2 conditions. This behavior was already observed before in chapter 3.1.1 and originates from the utilized glassy carbon electrode. The blank experiment with glassy carbon (Figure 34 (b)) under the same conditions revealed that the current density was nearly 3 times higher under N_2 and up to 2 times higher under CO_2 conditions compared to Figure 34 (a), which indicated that the formed leucoemeraldine layer reduced the overall conductivity of the system. Referring to the paper of Hursán *et al.*[27], a chronoamperometry measurement was also conducted to determine the effect of the illumination onto the current output of the electrode, which is depicted in Figure 35.

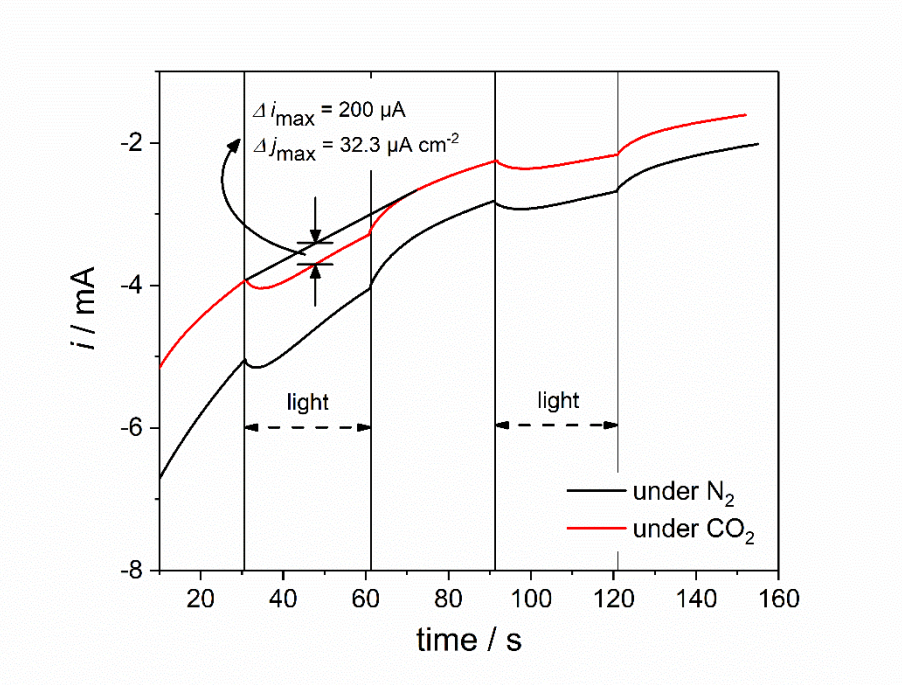

Figure 35: Chronoamperometry of PANI on GCE in 0.5 M potassium bicarbonate electrolyte at -1.3 V under N_2 and CO_2 and under alternating 30 seconds dark and 30 seconds illuminated (460 mW cm^{-2}) conditions.

The graph (Figure 35) shows the behavior of the current under dark and illuminated conditions, whereas it was visible that the current increased upon illumination under both N_2 and CO_2. The difference in the estimated dark and illuminated current was marked in the graph for CO_2 at the first cycle. Therefore, the gain in current density under illumination was estimated to be 32.3 µA cm^{-2}, which lies still below the maximum of 70 µA cm^{-2}, which was stated in the reference [27] under milder conditions.

A photoelectrolysis at - 1.3 V was conducted with the PANI/GCE electrode in 0.5 M potassium bicarbonate for 2 hours under CO_2 and the evolved species in the head space and the electrolyte solution were analyzed. This experiment was repeated at least three times to validate the outcome. Additionally, a single 20-hour photoelectrolysis was conducted under the same conditions to investigate the behavior over a long-time photoelectrolysis. The results of the faradaic efficiency for carbon monoxide and hydrogen evolution of these experiments are listed in Table 6.

Experiment	% FE for CO	% FE for H_2
2 hours – first	1.0	2.9
2 hours - second	3.0	3.0
2 hours - third	1.0	0.0
2 hours - forth	7.5	3.2
20 hours	1.3	4.2

Table 6: Electrochemical faradaic efficiency results of multiple conducted PANI/GCE photoelectrolysis experiments.

The results of all conducted experiments in Table 6 show the faradaic efficiency of carbon monoxide and hydrogen. The mean value and the standard deviation of all 2-hour experiments were calculated, which revealed 3.1 ± 2.7 % FE for CO and 2.3 ± 1.3 % FE H_2 respectively. Curiously enough, this result displays that it was possible to form CO with a polyaniline/glassy carbon electrode on a small-scale level. This was also confirmed by the results of the conducted 20-hour photoelectrolysis, which showed a similar trend. However, at the same time only little amounts of hydrogen were found, which leaves the question to where or in what process more than 90 % FE went. Since no additional analytes like methanol, ethanol, or formate were found to be present after the photoelectrolysis it was suggested that the electrons where utilized during the reduction of polyaniline or other side reactions. The following CV in Figure 36 shows the (photo-)electrochemical behavior of a PANI/GCE film before and after the photoelectrolysis under CO_2.

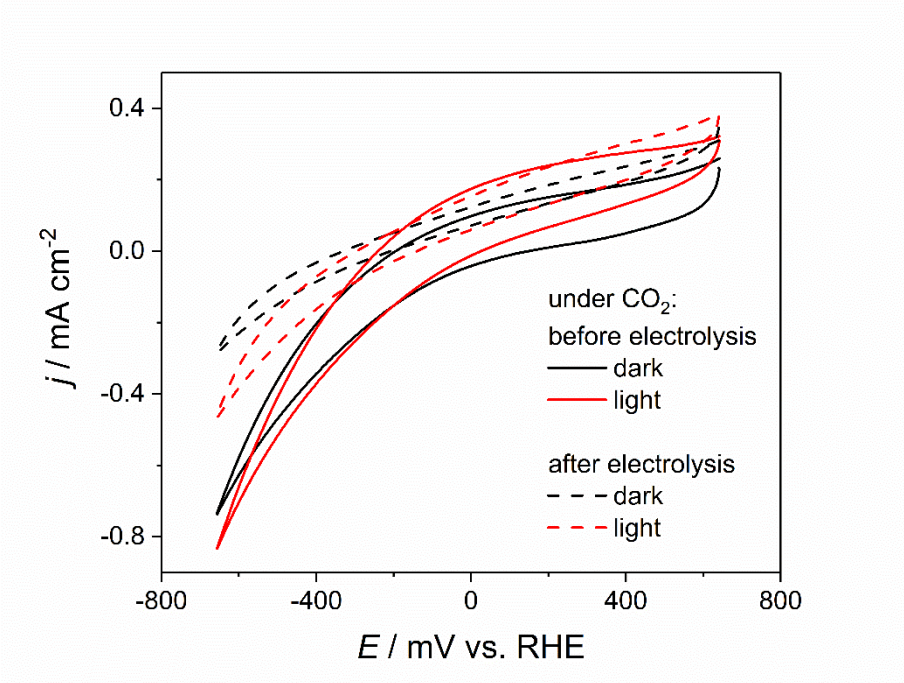

Figure 36: CV of PANI on GCE in 0.5 M potassium bicarbonate electrolyte in reductive potential before and after the photoelectrolysis under CO_2 and under dark and illumination.

It was observed from the graph in Figure 36 that the current density of the electrode was reduced by half after the photoelectrolysis, which indicated that the conductivity or the surface properties of the polymer film changed during this measurement. However, a photon-induced amplification of the current density was still noted after the photoelectrolysis, which was indicated by the red dotted graph, compared to the black dotted graph. A change of the polyaniline film during the CVs and after the photoelectrolysis was clearly visible with bare eyes, whereas the color changed from the known dark green to a blue/violet color. In addition, the area of illumination would become transparent throughout the excessive duration of the measurement. The change of the

appearance of the film is shown in Figure 37 for the PANI/GCE film after the 20-hour photoelectrolysis, which showed the same behavior in terms of looks as the 2-hour experiments.

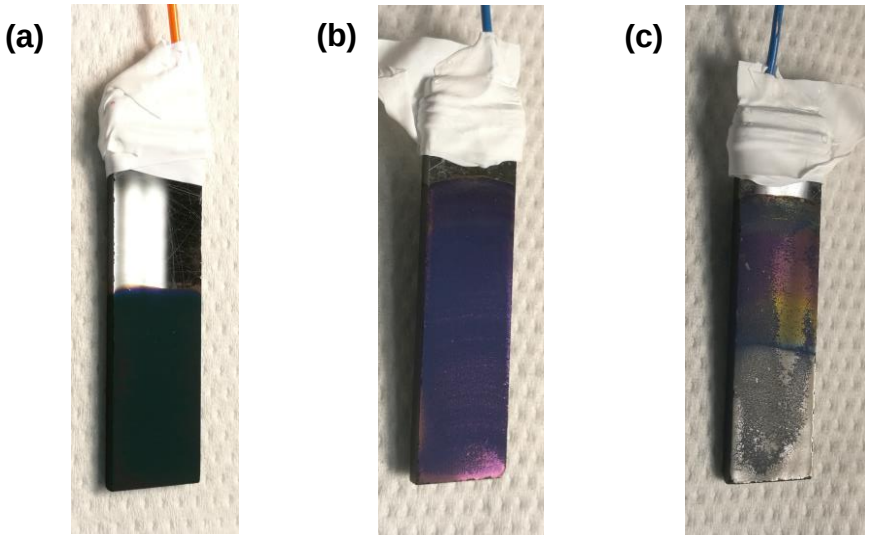

Figure 37: (a) Stages of a PANI/GCE electrode before the 20-hour photoelectrolysis (sample), (b) after the photolelectrolysis from the backside and (c) on the frontside with the notable illumination area.

The corresponding SEM images of the film before and after the 20-hour photoelectrolysis are depicted in Figure 38.

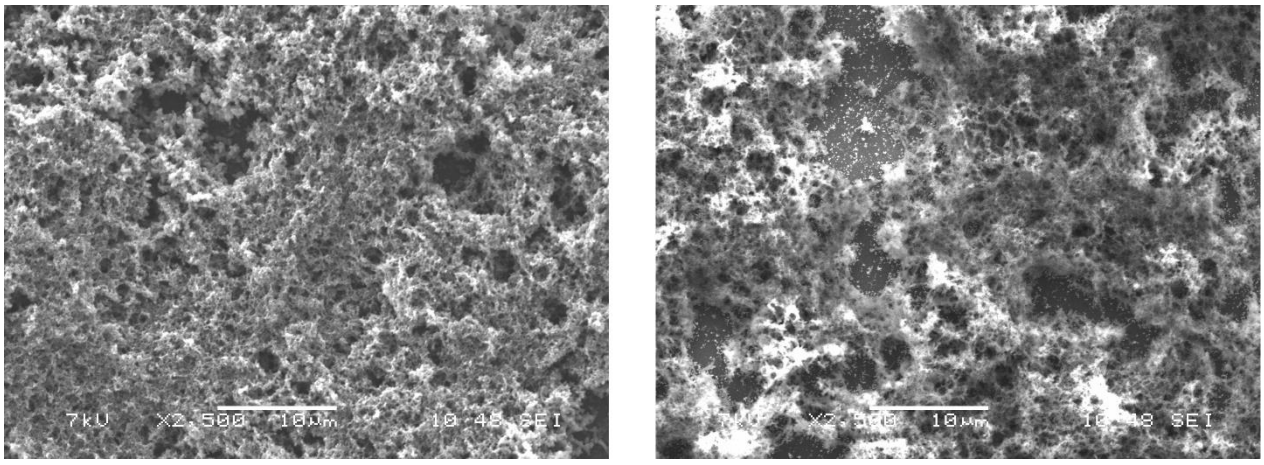

Figure 38: SEM surface images from the PANI/GCE before (left) and after the 20-hour photoelectrolysis (illuminated area) (right).

The SEM pictures in Figure 38 show the same PANI/GCE electrode with minor structural deviations before and after the conducted photoelectrolysis. No possible melting of the polymer was observed but moreover a slight loss of polyaniline, which was indicated by the formed canyons in the right picture that might occurred due to the highly applied reductive potential and the enhanced duration of the measurement and its applied conditions.

Several control experiments were conducted to validate that the observed CO evolution did not originate from a possible film degradation, or other effects. Therefore, an electrolysis with a PANI/GCE electrode was conducted without any illumination of the substrate under CO_2 conditions, which showed no results for CO evolution and a 2.1 % FE for H_2. An additional experiment consisted of a photoelectrolysis with a PANI/GCE electrode under N_2 conditions, which also showed no tendencies of CO evolution and a minor % FE for H_2. Furthermore, a glassy carbon electrode without a film was measured under the same conditions (illumination, and under CO_2), whereas no CO and 12.4 % FE for H_2 was observed. This showed that the bare glassy carbon electrode produced 5 times more hydrogen than PANI/GCE. Nevertheless, no CO was observed at the same time. After these conducted control experiments, one could surely state that the previous reported production of CO only occurred under CO_2 and with a utilized PANI/GCE electrode, which left no further speculation that the chosen configuration of the experiment itself enables the product formation but rather the investigated material itself.

3.2.3. Electrodeposited copper islands on polyaniline

Since the formation of carbon monoxide in the utilized system was very small and the overall faradaic efficiency indicated that over 90 % of the introduced current was not used for any sort of detectable product formation, an additional endeavor was undertaken to increase the efficiency of the investigated system. An already well known and explored route for CO formation is the utilization of metal catalysts, which can enable the production of a wide variety of chemical species such as ethanol, methanol, formate, carbon monoxide, methane, etc. Various books and literature references can give an insight to what type of metal produces what type of product [86], whereas a common metal catalyst in previous mentioned publications for the production of alcohols was copper embedded into a polyaniline framework. Copper can produce a whole spectrum of chemical species [86],[87], whereas the copper(I)-oxide is known to produce mainly alcohols under certain conditions [88],[89]. Therefore, copper was chosen as a supportive metal catalyst to aid the already established PANI/GCE electrode configuration and possibly enhance the observed formation of CO.

This was done by a potentiostatic electropolymerization technique, which introduced copper islands onto a premade standard PANI/GCE electrode in a single cell compartment. The procedure of Luo *et al.*[72] was utilized, which required a 0.1 M Na_2SO_4 electrolyte with 10 mM concentration of $CuSO_4$ and an electropolymerization potential of - 361 mV vs. Ag/AgCl/3M KCl for 480 seconds. In addition, the solution was purged for 1 hour with N_2 before to avoid any form of side reactions during the polymerization. The utilized cell for the potentiostatic electropolymerization can be seen in Figure 39, as well as the resulting formation of copper islands on the PANI surface in the SEM picture.

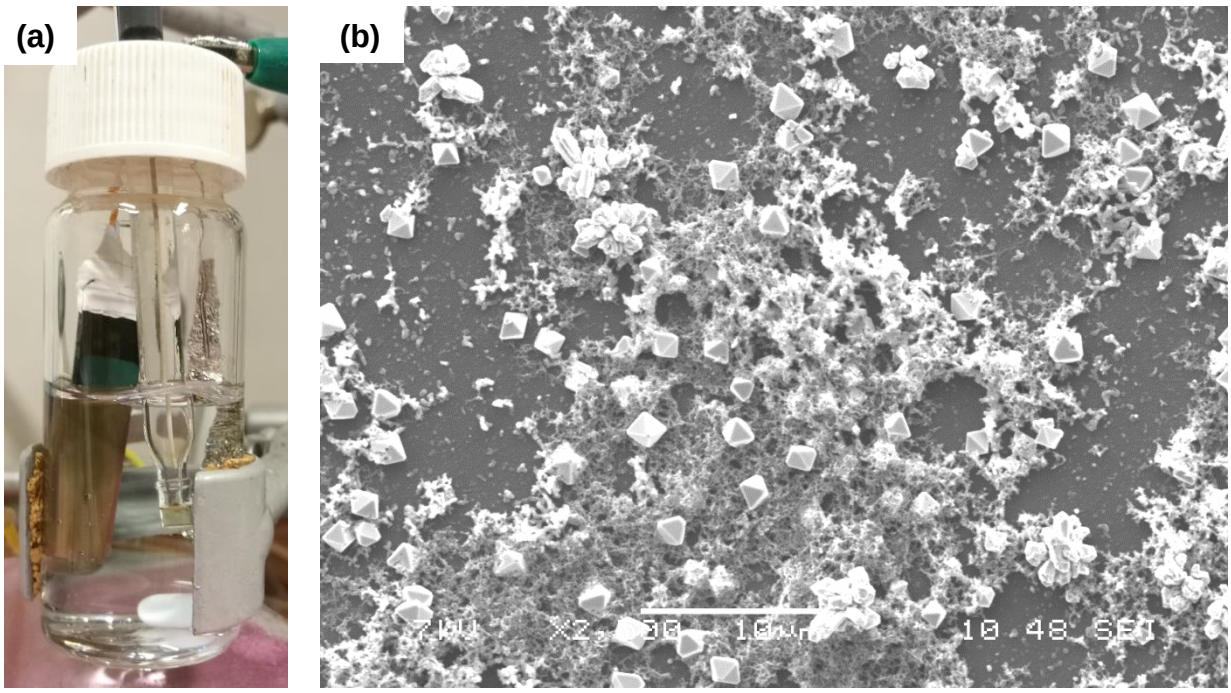

Figure 39: (a) Single cell compartment for the electrodeposition of copper onto PANI/GCE (WE) a Pt-foil (CE) and a Ag/AgCl/3M KCl (RE) in 0.1 M Na_2SO_4 with 10 mM $CuSO_4$. (b) SEM image of tetrahedral bipyramidal shaped copper islands on top of PANI/GCE.

The electrodeposition of copper onto PANI with the utilized setup in Figure 39 (a) was easy achievable and the results were reproduceable. It was noted that a thin brownish film was already observed after an electropolymerization duration of 240 seconds. The total duration of 480 seconds lead to the displayed copper islands in Figure 39 (b) with an average crystal size of 2 µm. The characterization of the Cu/PANI/GCE electrode was conducted in a similar way to the previous investigated PANI/GCE film to obtain comparable results, which included the photoelectrolysis at - 1.3 V vs. Ag/AgCl/3M KCl for 2 hours. The CV of the Cu/PANI/GCE electrode, plotted vs. RHE, under N_2 and CO_2 purged conditions and under illumination is depicted in Figure 40.

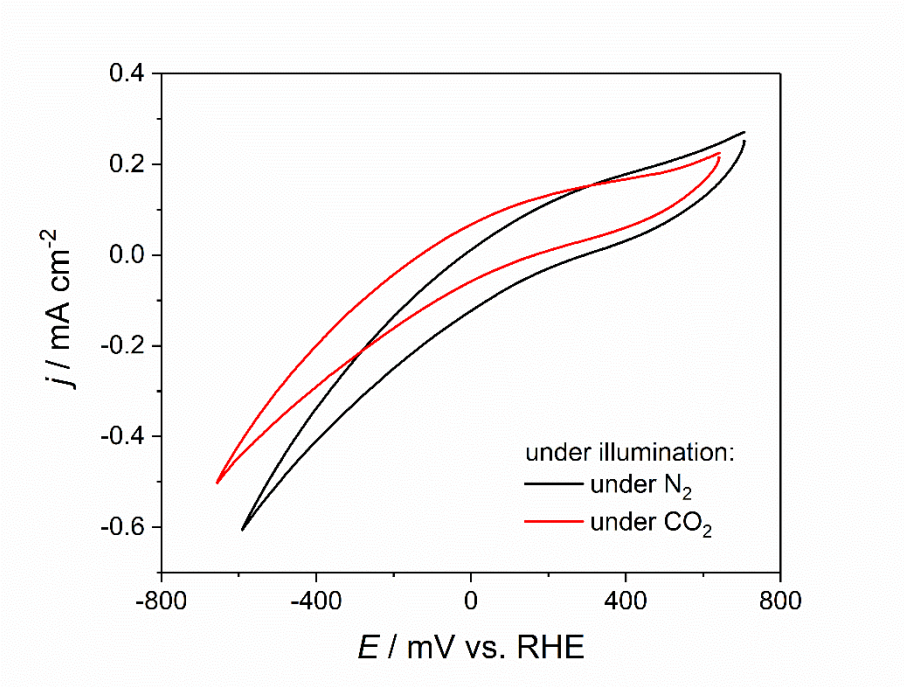

Figure 40: CV of Cu on PANI on GCE in 0.5 M potassium bicarbonate electrolyte in reductive potential under N_2 and CO_2 and under illumination with 460 mW cm^{-2}.

The CV in Figure 40 showed major similarities with Figure 34 (a) in terms of the absence of distinctive reduction or oxidation peaks, whereas it was clearly observed that the introduction of copper lead to a decrease of the current density up to nearly two times at - 0.65 V. The chronoamperometric measurement revealed an increase of the current density for the first CO_2 dark/light cycle of 43 µA cm^{-2}, which was overall higher as for the PANI/GCE electrode. This behavior was an effect of the additional introduced copper metal. The products of the 2-hour photoelectrolysis were again quantified, whereas a 0.6 % FE for CO and 35.0 % FE for H_2 evolution was discovered, without traces of any other analytes such as alcohols or formate. This showed that copper did not contribute to the carbon monoxide formation, as well as to the formation of other chemical species, which might be a side effect of the highly applied overpotential. In comparison to the PANI/GCE electrode, the high amount of hydrogen evolution was likely to originate from the introduced metal (copper), which enabled this process at such a rate because of the highly reductive potential during the photoelectrolysis.

The condition of the electrode after the photoelectrolysis was again checked by performing a CV under dark and illumination afterwards, which was compared to the measured post-electrolysis CVs in Figure 41.

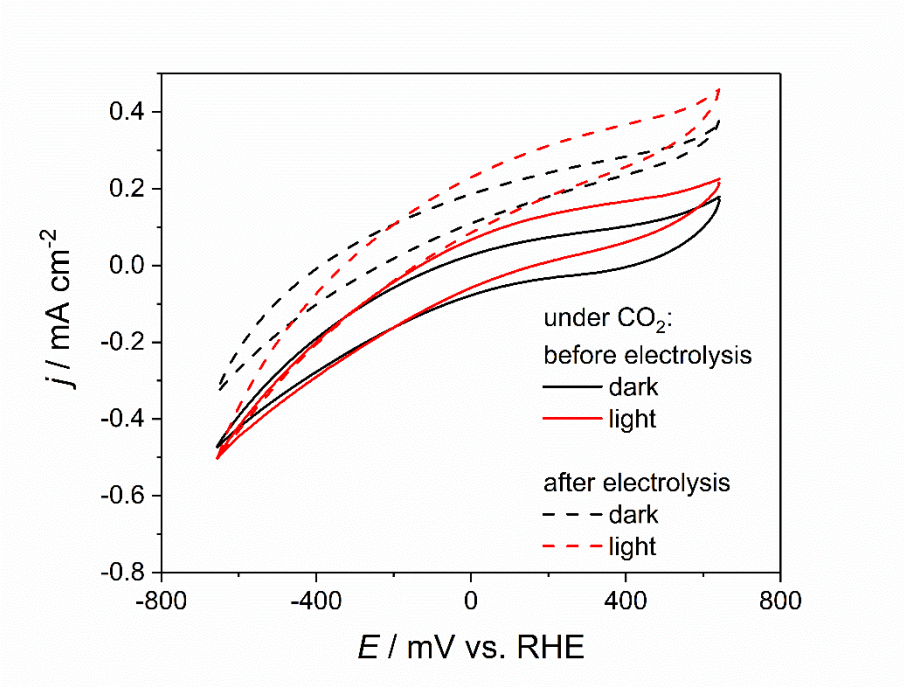

Figure 41: CV of Cu on PANI on GCE in 0.5 M potassium bicarbonate electrolyte in reductive potential before and after the photoelectrolysis under CO_2 and under dark and illumination.

The comparison of the CVs before and after the photoelectrolysis in Figure 41 showed a similar trend as already observed in Figure 36. However, it was especially observed for the Cu/PANI/GCE electrode that the current density at - 0.65 V stayed mainly the same before and after the photoelectrolysis under illumination. This effect was not observed under dark conditions, where the current density was reduced afterwards. Additionally, the CV with and without illumination after the photoelectrolysis (dotted graphs) started at a higher current density in the oxidative region, e.g. 0.46 mA cm^{-2} at 0.64 V (after) compared to 0.23 mA cm^{-2} at 0.64 V (before) both under illumination. This might be the effect of a prior reduced species, which was then again oxidized at a higher positive current flow.

4. Conclusion

The focus in this work was set on the heterogeneous carbon dioxide reduction with organic pigments and conductive polymers in aqueous electrolyte solution, as well as exploration of possible combination mechanisms of both materials. It was determined that the evaporated perylene derivatives films (PTCDA, H_2PTCDI, and Diphy-PTCDI) on Cr-Au- and glassy carbon electrodes, inherited no CO_2 capture properties under the utilized experimental conditions by being investigated via cyclic voltammetry in organic and aqueous electrolyte solutions.

A route to facilitate a bilayer-arrangement of a polyaniline layer on top of H_2PTCDI was electrochemically analyzed, whereas stability issues were encountered likely because of the harsh acidic conditions in which PANI was synthesized onto the perylene film. Further efforts were raised to electro-co-polymerize polyaniline and PTCDA/H_2PTCDI in basic and acidic conditions onto Cr-Au- and glassy carbon electrodes. The electrochemical behavior of these films was characterized in 0.1 M phosphate buffer, which revealed no properties towards carbon dioxide reduction nor capture. However, it was observed that films of PTCDA and H_2PTCDI could be casted electrochemically onto substrates from material-loaded 0.1 M KOH solutions. These films revealed similar characteristics as their evaporated films.

The catalytic properties of bulk-PANI/GCE electrodes were photoelectrochemically studied in aqueous electrolyte solution. No formation of alcohols or formate could be found, although identical conditions were utilized as in the suggested literature [27], which suggests that the results of said work group are incorrect or incomplete. Further improvements to the experimental conditions, such as the increase of applied voltage, usage of CO_2-rich electrolyte solutions, and a more powerful lamp for illumination revealed a tendency of PANI to produce CO (3.1 ± 2.7 % FE) and H_2 (2.3 ± 1.3 % FE) with no other formed products. Multiple experiments were conducted to verify this result, as well as a 20-hour long-time photoelectrolysis. In addition, various blank experiments were arranged to exclude possible electrocatalytic effects from the used setup. Moreover, copper islands were electrodeposited onto such bulk-PANI/GCE electrodes and measured under the same conditions. The addition of metal showed an improvement of hydrogen evolution (35.0 % FE) but no relevant increase in CO (0.6 % FE) or other possible formed products.

The behavior of the electrodes after the photoelectrolysis was explored, whereas it was noted that the current-density of the system was heavily decreased, which is attributed to the minor loss of material and possible loss of conductivity because of the harsh experimental conditions (high applied voltage, powerful illumination).

5. References

[1] Overbye, D., Far-Off Planets Like the Earth Dot the Galaxy,. *The New York Times*. November 4, 2013.

[2] Petigura, E. A.; Howard, A. W.; Marcy, G. W., Prevalence of Earth-Size Planets Orbiting Sun-like Stars,. *Proc. Natl. Acad. Sci.*, **2013**, *110* (48), 19273–19278.

[3] Prasad, P. V. V.; Thomas, J. M. G.; Narayanan, S., Global Warming Effects,. In *Encyclopedia of Applied Plant Sciences*; Elsevier, 2017; pp 289–299.

[4] Cao, J.; Zhao, B.; Gao, L.; Li, J.; Li, Z.; Zhao, X., Increasing Temperature Sensitivity Caused by Climate Warming, Evidence from Northeastern China,. *Dendrochronologia*, **2018**, *51*, 101–111.

[5] Winter, R. A., Innovation and the Dynamics of Global Warming,. *J. Environ. Econ. Manage.*, **2014**, *68* (1), 124–140.

[6] Tuckett, R., Greenhouse Gases,. *Ref. Modul. Chem. Mol. Sci. Chem. Eng.*, **2018**.

[7] Scripps Institution of Oceanography https://scripps.ucsd.edu/programs/keelingcurve/ (accessed Feb 25, 2019).

[8] Archer, D.; Eby, M.; Brovkin, V.; Ridgwell, A.; Cao, L.; Mikolajewicz, U.; Caldeira, K.; Matsumoto, K.; Munhoven, G.; Montenegro, A.; et al., Atmospheric Lifetime of Fossil Fuel Carbon Dioxide,. *Annu. Rev. Earth Planet. Sci*, **2009**, *37*, 117–134.

[9] Archer, D.; Brovkin, V., The Millennial Atmospheric Lifetime of Anthropogenic CO_2,. In *Climatic Change*; Springer Verlag, 2008; Vol. 90, pp 283–297.

[10] Archer, D., Fate of Fossil Fuel CO_2 in Geologic Time,. *J. Geophys. Res. C Ocean.*, **2005**, *110* (9), 1–6.

[11] Prăvălie, R.; Patriche, C.; Bandoc, G., Spatial Assessment of Solar Energy Potential at Global Scale. A Geographical Approach,. *J. Clean. Prod.*, **2019**, *209*, 692–721.

[12] Wu, J.; Huang, Y.; Ye, W.; Li, Y., CO_2 Reduction: From the Electrochemical to Photochemical Approach,. *Adv. Sci.*, **2017**, *4* (11), 1–29.

[13] Metz, B.; Davidson, O.; De Coninck, H. C.; Loss, M.; Meyer, L. A., *Carbon Dioxide Capture and Storage*; Cambridge University Press, 2005.

[14] Al-mamoori, A.; Krishnamurthy, A.; Rownaghi, A. A.; Rezaei, F., Carbon Capture and Utilization Update,. *Energy Technol.*, **2017**, *5* (6), 1–17.

[15] Riduan, S. N.; Zhang, Y., Recent Developments in Carbon Dioxide Utilization under Mild Conditions,. *Dalt. Trans.*, **2010**, *39*, 3347–3357.

[16] Sun, Z.; Ma, T.; Tao, H.; Fan, Q.; Han, B., Fundamentals and Challenges of Electrochemical CO_2 Reduction Using Two-Dimensional Materials,. *CHEMPR*, **2017**, *3* (4), 560–587.

[17] Lu, Q.; Jiao, F., Electrochemical CO_2 Reduction: Electrocatalyst, Reaction Mechanism, and Process Engineering,. *Nano Energy*, **2016**, *29*, 439–456.

[18] Zoski, C., *Handbook of Electrochemistry*; Elsevier, 2007.

[19] Lehn, J.-M.; Ziessel, R., Photochemical Generation of Carbon Monoxide and Hydrogen by Reduction of Carbon Dioxide and Water under Visible Light Irradiation,. *Proc. Natl. Acad. Sci.*, **1982**, *79* (2), 701–704.

[20] Hawecker, J.; Lehn, J.-M.; Ziessel, R., Efficient Photochemical Reduction of CO_2 to CO by Visible Light Irradiation of Systems Containing $Re(Bipy)(CO)_3X$ or $Ru(Bipy)_3^{2+}$ – Co^{2+} Combinations as Homogeneous Catalysts,. *J. Chem. Soc., Chem. Commun.*, **1983**, No. 9, 536–538.

[21] Hawecker, J.; Lehn, J.; Ziessel, R., Electrocatalytic Reduction of Carbon Dioxide Mediated by $Re(Bipy)(CO)_3Cl$ (Bipy = 2,2′-Bipyridine),. *J. Chem. Soc., Chem. Commun.*, **1984**, *984* (6), 328–330.

[22] Sullivan, B. P.; Bolinger, C. M.; Conrad, D.; Vining, W. J.; Meyer, T. J., One- and Two-Electron Pathways in the Electrocatalytic Reduction of CO_2 by $Fac\text{-}Re(Bpy)(CO)_3Cl$ (Bpy = 2,2′-Bipyridine),. *J. Chem. Soc., Chem. Commun.*, **1985**, *985* (20), 1414–1416.

[23] M. Michalska, Z.; E. Webster, D., Supported Homogeneous Catalysts,. *Appl. Catal.*, **1974**, *18* (2), 65–73.

[24] Aydin, R.; Köleli, F., Electrochemical Reduction of CO_2 on a Polyaniline Electrode under Ambient Conditions and at High Pressure in Methanol,. *J. Electroanal. Chem.*, **2002**, *535* (1–2), 107–112.

[25] Köleli, F.; Röpke, T.; Hamann, C. H., The Reduction of CO_2 on Polyaniline Electrode in a Membrane Cell,. *Synth. Met.*, **2004**, *140* (1), 65–68.

[26] Liu, G.; Bai, H.; Zhang, B.; Peng, H., Role of Organic Components in Electrocatalysis for Renewable Energy Storage,. *Chem. - A Eur. J.*, **2018**, *24* (69), 18271–18292.

[27] Hursán, D.; Kormányos, A.; Rajeshwar, K.; Janáky, C., Polyaniline Films Photoelectrochemically Reduce CO_2 to Alcohols,. *Chem. Commun.*, **2016**, *52* (57), 8858–8861.

[28] Hori, Y., Electrochemical CO_2 Reduction on Metal Electrodes,. In *Modern Aspects of Electrochemistry*; Springer New York: New York, NY, 2008; Vol. 42, pp 89–189.

[29] Ogura, K.; Endo, N.; Nakayama, M.; Ootsuka, H., Mediated Activation and Electroreduction of CO_2 on Modified Electrodes with Conducting Polymer and Inorganic Conductor Films,. *J. Electrochem. Soc.*, **1995**, *142* (12), 4026.

[30] Grace, A. N.; Choi, S. Y.; Vinoba, M.; Bhagiyalakshmi, M.; Chu, D. H.; Yoon, Y.; Nam, S. C.; Jeong, S. K., Electrochemical Reduction of Carbon Dioxide at Low Overpotential on a Polyaniline/Cu_2O Nanocomposite Based Electrode,. *Appl. Energy*, **2014**, *120*, 85–94.

[31] Dodabalapur, A.; Katz, H. E.; Torsi, L., Molecular Orbital Energy Level Engineering in Organic Transistors,. *Adv. Mater.*, **1996**, *8* (10), 853–855.

[32] Schön, J. H.; Kloc, C.; Batlogg, B., Perylene: A Promising Organic Field-Effect Transistor Material,. *Appl. Phys. Lett.*, **2000**, *77* (23), 3776–3778.

[33] Tang, C. W., Two-layer Organic Photovoltaic Cell,. *Appl. Phys. Lett.*, **1986**, *48* (2), 183–

185.

[34] Zafer, C.; Kus, M.; Turkmen, G.; Dincalp, H.; Demic, S.; Kuban, B.; Teoman, Y.; Icli, S., New Perylene Derivative Dyes for Dye-Sensitized Solar Cells,. *Sol. Energy Mater. Sol. Cells*, **2007**, *91* (5), 427–431.

[35] Li, J.-X.; Li, Z.-J.; Ye, C.; Li, X.-B.; Zhan, F.; Fan, X.-B.; Li, J.; Chen, B.; Tao, Y.; Tung, C.-H.; et al., Visible Light-Induced Photochemical Oxygen Evolution from Water by 3,4,9,10-Perylenetetracarboxylic Dianhydride Nanorods as an n-Type Organic Semiconductor,. *Catal. Sci. Technol.*, **2016**, *6* (3), 672–676.

[36] Apaydin, D. H.; Gora, M.; Portenkirchner, E.; Oppelt, K. T.; Neugebauer, H.; Jakesova, M.; Eric, D. G.; Kunze-liebha, J., Electrochemical Capture and Release of CO_2 in Aqueous Electrolytes Using an Organic Semiconductor Electrode,. *ACS Appl. Mater. Interfaces*, **2017**, *9* (15), 12919–12923.

[37] Liao, Y.; Weber, J.; Faul, C. F. J., Fluorescent Microporous Polyimides Based on Perylene and Triazine for Highly CO_2 - Selective Carbon Materials,. *Macromolecules*, **2015**, *48* (7), 2064–2073.

[38] Rao, K. V.; Haldar, R.; Kulkarni, C.; Maji, T. K.; George, S. J., Perylene Based Porous Polyimides: Tunable, High Surface Area with Tetrahedral and Pyramidal Monomers,. *Chem. Mater.*, **2012**, *24* (6), 969–971.

[39] Danziger, J.; Dodelet, J. P.; Armstrong, N. R., Electrochemical and Photoelectrochemical Processes on Thin Films of Perylenetetracarboxylic Dianhydride,. *Chem. Mater.*, **1991**, *3* (5), 812–820.

[40] Lee, S. K.; Zu, Y.; Herrmann, A.; Geerts, Y.; Müllen, K.; Bard, A. J., Electrochemistry, Spectroscopy and Electrogenerated Chemiluminescence of Perylene, Terrylene, and Quaterrylene Diimides in Aprotic Solution,. *J. Am. Chem. Soc.*, **1999**, *121* (14), 3513–3520.

[41] Rasmussen, S. C., The Early History of Polyaniline: Discovery and Origins,. *An Int. J. Hist. Chem. Subst.*, **2017**, *1* (12), 99–109.

[42] McNeill, R.; Siudak, R.; Wardlaw, J.; Weiss, D., Electronic Conduction in Polymers. I. The Chemical Structure of Polypyrrole,. *Aust. J. Chem.*, **1963**, *16* (6), 1056.

[43] Bolto, B.; Weiss, D., Electronic Conduction in Polymers. II. The Electrochemical Reduction of Polypyrrole at Controlled Potential,. *Aust. J. Chem.*, **1963**, *16* (6), 1076.

[44] Bolto, B.; McNeill, R.; Weiss, D., Electronic Conduction in Polymers. III. Electronic Properties of Polypyrrole,. *Aust. J. Chem.*, **1963**, *16* (6), 1090.

[45] Unverdorben, O., Ueber Das Verhalten Der Organischen Körper in Höheren Temperaturen,. *Ann. Phys.*, **1826**, *84* (11), 397–410.

[46] Runge, F. F., Ueber Einige Produkte Der Steinkohlendestillation,. *Ann. der Phys. und Chemie*, **1834**, *107* (5), 65–78.

[47] Fritsche, J., Ueber Das Anilin, Ein Neues Zersetzungsproduct Des Indigo,. *J. für Prakt. Chemie*, **1840**, *20* (1), 453–459.

[48] Zinin, N., Beschreibung Einiger Neuer Organischer Basen, Dargestellt Durch Die Einwirkung Des Schwefelwasserstoffes Auf Verbindungen Der Kohlenwasserstoffe Mit Untersalpetersäure,. *J. für Prakt. Chemie*, **1842**, *27* (1), 140–153.

[49] Hofmann, A. W., Chemische Untersuchung Der Organischen Basen Im Steinkohlen-Theeröl,. *Ann. der Chemie und Pharm.*, **1843**, *47* (1), 37–87.

[50] Lightfoot, J., The Chemical History and Progress of Aniline Black,. **1871**, 1–43.

[51] Runge, F. F., Ueber Einige Producte Der Steinkohlendestillation,. *Ann. der Phys. und Chemie*, **1834**, *107* (33), 513–524.

[52] Travis, A. S., From Manchester to Massachusetts via Mulhouse: The Transatlantic Voyage of Aniline Black,. *Technol. Cult.*, **1994**, *35* (1), 70.

[53] Travis, A. S., Artificial Dyes in John Lightfoot's Broad Oak Laboratory,. *Ambix*, **1995**, *42* (1), 10–27.

[54] Crace Calvert, F., *Lectures on Coal Tar Colours, and on Recent Improvements and Progress in Dyeing and Calico Printing*; Philadelphia, H.C. Baird: Manchester, 1863.

[55] Noelting, E., *Scientific and Industrial History of Aniline Black*; Wm. J. Matheson & Co.: New York, 1889.

[56] Travis, A. S., Heinrich Caro at Roberts, Dale & CO.,. *Ambix*, **1991**, *38* (3), 113–134.

[57] Letheby, H., On the Production of a Blue Substance by the Electrolysis of Sulphate of Aniline,. *J. Chem. Soc.*, **1862**, *15* (161), 161–163.

[58] Green, A. G.; Woodhead, A. E., Aniline-Black and Allied Compounds. Part I,. *J. Chem. Soc., Trans.*, **1910**, *97*, 2388–2403.

[59] Green, A. G.; Wolff, S., Anilinschwarz Und Seine Zwischenkörper,. *Berichte der Dtsch. Chem. Gesellschaft*, **1911**, *44* (3), 2570–2582.

[60] Green, A. G.; Woodhead, A. E., CXVII.—Aniline-Black and Allied Compounds. Part II,. *J. Chem. Soc., Trans.*, **1912**, *101*, 1117–1123.

[61] Fritzsche, J., Vorläufige Notiz Über Einige Neue Körper Aus Der Indigoreihe,. *J. für Prakt. Chemie*, **1843**, *28* (1), 198–204.

[62] Geniès, E. M.; Boyle, A.; Lapkowski, M.; Tsintavis, C., Polyaniline: A Historical Survey,. *Synth. Met.*, **1990**, *36* (2), 139–182.

[63] Feast, W. J.; Tsibouklis, J.; Pouwer, K. L.; Groenendaal, L.; Meijer, E. W., Synthesis, Processing and Material Properties of Conjugated Polymers,. *Polymer (Guildf).*, **1996**, *37* (22), 5017–5047.

[64] MacDiarmid, A. G.; Epstein, A. J., Conducting Polymers: Past, Present and Future…,. *MRS Proc.*, **1993**, *328*, 133.

[65] Bhadra, S.; Khastgir, D.; Singha, N. K.; Lee, J. H., Progress in Preparation, Processing and Applications of Polyaniline,. *Prog. Polym. Sci.*, **2009**, *34* (8), 783–810.

[66] Wallace, G.; Spinks, G.; Kane-Maguire, L.; Teasdale, P., *Conductive Electroactive Polymers*; CRC Press, 2008.

[67] Boeva, Z. A.; Sergeyev, V. G., Polyaniline: Synthesis, Properties, and Application,. *Polym. Sci. Ser. C*, **2014**, *56* (1), 144–153.

[68] Gvozdenovic, M.; Jugovic, B.; Stevanovic, J.; Trisovic, T.; Grgur, B., Electrochemical Polymerization of Aniline,. In *Electropolymerization*; InTech, 2011.

[69] Hussain, A. M. P.; Kumar, A., Electrochemical Synthesis and Characterization of Chloride Doped Polyaniline,. *Bull. Mater. Sci.*, **2003**, *26* (3), 329–334.

[70] Gvozdenovic, M.; Jugovic, B.; Stevanovic, J.; Grgur, B., Electrochemical Synthesis of Electroconducting Polymers,. *Hem. Ind.*, **2014**, *68* (6), 673–684.

[71] Ansari, R.; Keivani, M. B., Polyaniline Conducting Electroactive Polymers Thermal and Environmental Stability Studies,. *E-Journal Chem.*, **2006**, *3* (4), 202–217.

[72] Luo, J.; Jiang, S.; Zhang, H.; Jiang, J.; Liu, X., A Novel Non-Enzymatic Glucose Sensor Based on Cu Nanoparticle Modified Graphene Sheets Electrode,. *Anal. Chim. Acta*, **2012**, *709*, 47–53.

[73] Mazhar, M.; Abdouss, M.; Gharanjig, K.; Teimuri-Mofrad, R., Synthesis, Characterization and near Infra-Red Properties of Perylenebisimide Derivatives,. *Prog. Org. Coatings*, **2016**, *101*, 297–304.

[74] Kolhe, N. B.; Asha, S. K.; Senanayak, S. P.; Narayan, K. S., N-Type Field Effect Transistors Based on Rigid Rod and Liquid Crystalline Alternating Copoly(Benzobisoxazole) Imides Containing Perylene and/or Naphthalene,. *J. Phys. Chem. B*, **2010**, *114* (50), 16694–16704.

[75] Wielend, D.; Apaydin, D. H.; Sariciftci, N. S., Anthraquinone Thin-Film Electrodes for Reversible CO_2 Capture and Release,. *J. Mater. Chem. A*, **2018**, *6* (31), 15095–15101.

[76] Hauptmann, S., *Organische Chemie*, 2nd Editio.; VEB Deutscher Verlag für Grundstoffindustrie: Leibzig, 1985.

[77] Morávková, Z.; Dmitrieva, E., Structural Changes in Polyaniline near the Middle Oxidation Peak Studied by in Situ Raman Spectroelectrochemistry,. *J. Raman Spectrosc.*, **2017**, *48* (9), 1229–1234.

[78] Sapurina, I. Y.; Shishov, M. A., Oxidative Polymerization of Aniline: Molecular Synthesis of Polyaniline and the Formation of Supramolecular Structures,. In *New Polymers for Special Applications*; InTech, 2012.

[79] Langhals, H.; Karolin, J.; Johansson, L. B. ., Spectroscopic Properties of New and Convenient Standards for Measuring Fluorescence Quantum Yields,. *J. Chem. Soc. Faraday Trans.*, **1998**, *94* (19), 2919–2922.

[80] IR of 3,4,9,10-perylenetetracarboxylic dianhydrid in KBr disc https://sdbs.db.aist.go.jp/sdbs/cgi-bin/landingpage?spcode=IR-NIDA-18815 (accessed Mar 12, 2019).

[81] Zhanpeisov, N. U.; Nishio, S.; Fukumura, H., Density Functional Theory Study of Vibrational Properties of the 3,4,9,10-Perylene Tetracarboxylic Dianhydride (PTCDA) Molecule: IR,

Raman, and UV-Vis Spectra,. *Int. J. Quantum Chem.*, **2005**, *105* (4), 368–375.

[82] Shulitski, B. G.; Filippov, V. V., IR Absorption Anisotropy in Perylene-3,4,9,10-Tetracarboxylic Acid Dianhydride,. *J. Appl. Spectrosc.*, **2009**, *76* (5), 660–666.

[83] Pérez-Salado Kamps, Á.; Meyer, E.; Rumpf, B.; Maurer, G., Solubility of CO_2 in Aqueous Solutions of KCl and in Aqueous Solutions of K_2CO_3,. *J. Chem. Eng. Data*, **2007**, *52* (3), 817–832.

[84] Kobayashi, T.; Yoneyama, H.; Tamura, H., Oxidative Degradation Pathway of Polyaniline Film Electrodes,. *J. Electroanal. Chem. Interfacial Electrochem.*, **1984**, *177* (1–2), 293–297.

[85] Buron, C. C.; Lakard, B.; Monnin, A. F.; Moutarlier, V.; Lakard, S., Elaboration and Characterization of Polyaniline Films Electrodeposited on Tin Oxides,. *Synth. Met.*, **2011**, *161* (19–20), 2162–2169.

[86] Qiao, J.; Liu, Y.; Hong, F.; Zhang, J., A Review of Catalysts for the Electroreduction of Carbon Dioxide to Produce Low-Carbon Fuels,. *Chem. Soc. Rev.*, **2014**, *43* (2), 631–675.

[87] Gattrell, M.; Gupta, N.; Co, A., A Review of the Aqueous Electrochemical Reduction of CO_2 to Hydrocarbons at Copper,. *J. Electroanal. Chem.*, **2006**, *594* (1), 1–19.

[88] Le, M.; Ren, M.; Zhang, Z.; Sprunger, P. T.; Kurtz, R. L.; Flake, J. C., Electrochemical Reduction of CO_2 to CH_3OH at Copper Oxide Surfaces,. *J. Electrochem. Soc.*, **2011**, *158* (5), E45.

[89] Kas, R.; Kortlever, R.; Milbrat, A.; Koper, M. T. M.; Mul, G.; Baltrusaitis, J., Electrochemical CO_2 Reduction on Cu_2O-Derived Copper Nanoparticles: Controlling the Catalytic Selectivity of Hydrocarbons,. *Phys. Chem. Chem. Phys.*, **2014**, *16* (24), 12194–12201.